About the dynamics of a common class of activated sludge plants

Otacílio B. L. Neto[a,*], Michela Mulas[a] and Francesco Corona[a,b]

[a]Postgraduate Programme in Teleinformatics Engineering, Federal University of Ceará, Brazil
[b]School of Chemical Engineering, Aalto University, Finland

ARTICLE INFO

Keywords:
Activated sludge process
Stability
Controllability
Observability
Structural control
Complex networks

ABSTRACT

In this work, the stability, controllability and observability properties of a class of activated sludge plants are analysed. Specifically, the five biological reactors and the secondary settler in the Benchmark Simulation Model no. 1 (BSM1) are studied. For the task, we represented the plant as a dynamical system consisting of 145 state variables, 13 controls, 14 disturbances and 15 outputs and as a complex networks to study its full-state controllability and observability properties from a structural and a classical point of view. By analysing the topology of the network, we show how this class of systems is controllable but not observable in a structural sense, and thus how it is controllable but not observable in a classical sense for almost all possible realisations. We also show how a linearisation commonly used in the literature is neither full-state controllable nor full-state observable in the classical sense. The control and observation efforts are quantified in terms of energy- and centrality-based based metrics.

1. Introduction

Stricter effluent requirements, costs minimisation, sustainable water and energy cycles, recovery of nutrients and other resources, as well as increasing expectations in the public to attain high service standards require wastewater treatment to face unprecedented operational challenges. Because of their wide diffusion, activated sludge processes play a central role in the biological treatment of wastewater and their efficient management has a large technological and societal impact.

Many control strategies for activated sludge plants have been proposed in the industrial and academic literature. More than forty years ago the first specialised conference on Instrumentation, Control and Automation of Water and Wastewater systems was founded with the firm goal of encouraging the application of automation technologies to wastewater treatment plants. Pioneering works, as Olsson et al. (1973) and Olsson and Andrews (1978), inspired numerous researchers and practitioners to approach this specific field. Extensive reviews of the various control solutions can be found in Olsson et al. (2005, 2013). Importantly, many research efforts have been fostered thanks to a number of support tools that provide a simulation protocol for real-world activated sludge processes. The Benchmark Simulation Model no. 1 (BSM1, Gernaey et al. (2014)), specifically, singled out as the reference platform for developing and controlling activated sludge processes subjected to typical municipal wastewater influents.

The availability of the BSMs has led to the design of many modelling and control solutions (Alex et al., 2002; Rosen et al., 2002; Stare et al., 2007; Holenda et al., 2008; Ostace et al., 2011; Åmand et al., 2013; Han et al., 2014; Francisco et al., 2015; Zeng and Liu, 2015; Zhang and Liu, 2019; Moliner-Heredia et al., 2019), which, regretfully, have not yet been digested in a comprehensive review. These works, while remarkable in addressing specific control objectives, highlight the necessity to further understand BSM-like systems from a control theoretical perspective. System properties like stability, controllability and observability of BSMs have been touched only marginally or studied only for simpler subsystems. In Benazzi and Katebi (2005), the nonlinear global observability of a single bio-reactor from the plant is analysed. Busch et al. (2013) discusses optimal measurement configurations that ensure local observability for a BSM1 in which the settler's model is simplified. In Zeng et al. (2016), the same simplified model is decomposed into subsystems which are then each tested for observability, individually. Works like Yin and Liu (2018), Yin et al. (2018) and Yin and Liu (2019) systematically exploit the notion of observability to either design state estimators, subsystem decompositions, or to test this property for the BSM1 model, though under a rather unrealistically large set of measurements. To the best of our knowledge, no similar studies report on the stability and controllability properties. Under this scenario, this work aims at contributing to the understanding of a large class of activated sludge plants by analysing the stability, controllability and observability properties of this important benchmark.

For the analysis, the dynamical system associated with the BSM1 is mapped onto a complex network where its full-state controllability and observability properties are studied. As we have been interested in determining whether the system is controllable and observable under all feasible linearisations (Neto et al., 2020a,b), we couple classical control notions from linear system theory (Callier and Desoer, 1991) with graph-theoretic tools (Lin, 1974; Mayeda and Yamada, 1979; Reinschke, 1988; Liu et al., 2011; Jarczyk et al., 2011; Liu et al., 2013; Jia et al., 2021). This allows us to determine such properties from the structure of the graph, regardless of the linearisation. The classical analysis is performed on a linearisation of the BSM1 often encountered in the literature.

Our analyses show that activated sludge plants described using the BSM1 are structurally controllable, but that they are not structurally observable. Because of the generality of this

*Corresponding author
ORCID(s):

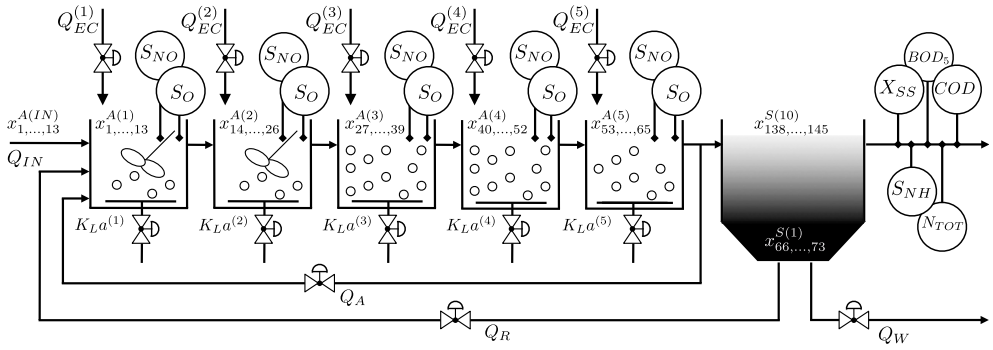

Figure 1: The activated sludge plant: Process layout.

result, we implicitly show also how the BSM1 is full-state controllable but not full-state observable in a classical sense, for almost all possible linearisations of the model. In addition, the conditions to satisfy the more restrictive notions of strong structural controllability and observability are not satisfied. The classical counterpart of this result is verified with Popov-Belevitch-Hautus tests (Hautus, 1970). An important result of our analysis is that a common linearisation of the BSM1 is not full-state controllable and not full-state observable. Being controllability and observability notions of the binary type, we complement the analysis by determining also the energy- and centrality-based metrics (Müller and Weber, 1972; Pasqualetti et al., 2014; Summers et al., 2016) which quantify the control and observation efforts that are needed to operate this class of wastewater treatment plants.

The analysis is presented as follows: Section 2 describes the activated sludge plant and its state-space model, Section 3 sets the preliminaries and the notation by overviewing the concepts of stability and the classical and structural notions of controllability and observability. Section 4 discusses our results on the stability, full-state controllability and observability for this class of activated sludge plants. In Section 5 we discuss the results for two alternative configurations of the plant. Model equations, model parameters, and the operating point used for linearisation are reported in Appendix A.

2. The activated sludge plant: Process overview and state-space model

We consider the activated sludge process in a conventional biological wastewater treatment plant. Based on the denitrification-nitrification process, bacteria reduce nitrogen present in the influent wastewater in the form of ammonia into nitrate, which is subsequently reduced into nitrogen gas to be released into the atmosphere. The prototypical process, in Fig. 1, consists of five biological reactors and a settler.

The treatment starts with a first reactor where wastewater from primary sedimentation, return sludge from secondary sedimentation and internal recycle sludge are fed. The outflow from the first reactor is then fed sequentially to the downstream reactors and, eventually, from the fifth reactor to the secondary settler. Mixed liquor from the fifth reactor is recirculated into the first reactor together with the recycle sludge from secondary sedimentation, as mentioned. Excess sludge from the settler can also be directed towards other processes. Oxygen can be added by insufflating air into each reactor. In the aerated reactors, the ammonium nitrogen (NH_4-N) in the wastewater is oxidised into nitrate nitrogen (NO_3-N), which is in turn reduced into nitrogen gas (N_2) in the anoxic reactors. An additional carbon source can be added to each rector independently. No other chemicals are added to the process.

Each reactor is described by the Activated Sludge Model no. 1 (Henze et al., 2000). For the settler, a 10-layers non-reactive model by Takács et al. (1991) is used. Under this setup, the process corresponds to the Benchmark Simulation Model no. 1 (Gernaey et al., 2014), or activated sludge plant (ASP).

The dynamics of each reactor $A(r)$ ($r = 1, \dots, 5$) are described by 13 state variables, the vector of concentrations

$$x^{A(r)} = (S_I^{A(r)}, S_S^{A(r)}, X_I^{A(r)}, X_S^{A(r)}, X_{BH}^{A(r)}, X_{BA}^{A(r)}, X_P^{A(r)}, S_O^{A(r)}, S_{NO}^{A(r)}, S_{NH}^{A(r)}, S_{ND}^{A(r)}, X_{ND}^{A(r)}, S_{ALK}^{A(r)})^\mathsf{T}, \quad (1)$$

and controllable inputs $u^{A(r)} = (K_La^{(r)}, Q_{EC}^{(r)})$, the oxygen transfer coefficient $K_La^{(r)}$ and external carbon source flow-rate $Q_{EC}^{(r)}$. The dynamics of each layer $S(l)$ ($l = 1, \dots, 10$) of the settler are described by 8 state variables, the vector

$$x^{S(l)} = (X_{SS}^{S(l)}, S_I^{S(l)}, S_S^{S(l)}, S_O^{S(l)}, S_{NO}^{S(l)}, S_{NH}^{S(l)}, S_{ND}^{S(l)}, S_{ALK}^{S(l)})^\mathsf{T}. \quad (2)$$

The plant is subjected to three additional controllable inputs, the internal and external sludge recycle flow-rates (Q_A and Q_R, respectively) and the wastage flow-rate Q_W, and to 14 disturbances, the influent flow-rate Q_{IN} and its concentrations $x^{A(IN)}$, all entering the first reactor. Wastewater concentrations in the internal recycle are given by $x^{A(5)}$, whereas $x^{S(1)}$ are concentrations in the external recycle and wastage.

As for the measurements, we consider a sensor-arrangement consisting of analysers determining the concentrations

$$y = (y^{A(1)}, \dots, y^{A(5)}, X_{SS}^{S(10)}, S_{NH}^{S(10)}, BOD_5^{S(10)}, COD^{S(10)}, N_{TOT}^{S(10)})^\mathsf{T}. \quad (3)$$

Table 1
Activated sludge plant: Process variables by location ('$A(r)$', $r = 1, \dots, 5$, in the r-th bio-reactor, or 'IN' in the influent wastewater; '$S(l)$', $l = 1, \dots, 10$, in the l-th settler layer) and type ('D', disturbance; 'S', state variable; 'M' measurement; and 'C', control).

Variable	Description	Type	Units
S_I^{IN}, $S_I^{A(r)}$, $S_I^{S(l)}$	Soluble inert organic matter	D, S, S	g COD m^{-3}
S_S^{IN}, $S_S^{A(r)}$, $S_S^{S(l)}$	Readily biodegradable substrate	D, S, S	g COD m^{-3}
X_I^{IN}, $X_I^{A(r)}$	Particulate inert organic matter	D, S	g COD m^{-3}
X_S^{IN}, $X_S^{A(r)}$	Slowly biodegradable substrate	D, S	g COD m^{-3}
X_{BH}^{IN}, $X_{BH}^{A(r)}$	Active heterotrophic biomass	D, S	g COD m^{-3}
X_{BA}^{IN}, $X_{BA}^{A(r)}$	Active autotrophic biomass	D, S	g COD m^{-3}
X_P^{IN}, $X_P^{A(r)}$	Particulate products from biomass decay	D, S	g COD m^{-3}
S_O^{IN}, $S_O^{A(r)}$, $S_O^{S(l)}$	Dissolved oxygen	D, S/M, S	g O_2 m^{-3}
S_{NO}^{IN}, $S_{NO}^{A(r)}$, $S_{NO}^{S(l)}$	Nitrate and nitrite nitrogen	D, S/M, S	g N m^{-3}
S_{NH}^{IN}, $S_{NH}^{A(r)}$, $S_{NH}^{S(l)}$	NH_4^++ NH_3 nitrogen	D, S, S/M($l = 10$)	g N m^{-3}
S_{ND}^{IN}, $S_{ND}^{A(r)}$, $S_{ND}^{S(l)}$	Soluble biodegradable organic nitrogen	D, S, S	g N m^{-3}
X_{ND}^{IN}, $X_{ND}^{A(r)}$	Particulate biodegradable organic nitrogen	D, S	g N m^{-3}
S_{ALK}^{IN}, $S_{ALK}^{A(r)}$, $S_{ALK}^{S(l)}$	Alkalinity	D, S	mol HCO_3^- m^{-3}
$X_{SS}^{S(l)}$	Total suspended solids	S/M($l = 10$)	g COD m^{-3}
Q_{IN}	Influent flow-rate	D	m^3 d^{-1}
Q_A	Internal recirculation flow-rate	C	m^3 d^{-1}
Q_R	External recirculation flow-rate	C	m^3 d^{-1}
Q_W	Wastage flow-rate	C	m^3 d^{-1}
$Q_{EC}^{(r)}$	External carbon source flow-rate	C	m^3 d^{-1}
$K_L a^{(r)}$	Oxygen transfer coefficient	C	d^{-1}
$BOD_5^{S(10)}$	Biochemical oxygen demand	M	g COD m^{-3}
$COD^{S(10)}$	Chemical oxygen demand	M	g COD m^{-3}
$N_{TOT}^{S(10)}$	Total nitrogen	M	g N m^{-3}

with $y^{A(r)} = \left(S_O^{A(r)}, S_{NO}^{A(r)}\right)$ the measurements taken at the r-th bio-reactor. The effluent concentrations of biochemical oxygen demand (BOD_5), chemical oxygen demand (COD) and total nitrogen (N_{TOT}) are defined from state variables,

$$BOD_5^{S(10)} = ((1 - f_P)(X_{BH}^{S(10)} + X_{BA}^{S(10)}) + S_S^{S(10)} + X_S^{S(10)})/4; \quad (4a)$$

$$COD^{S(10)} = S_S^{S(10)} + S_I^{S(10)} + X_S^{S(10)} + X_I^{S(10)} + X_{BH}^{S(10)} + X_{BA}^{S(10)} + X_P^{S(10)}; \quad (4b)$$

$$N_{TOT}^{S(10)} = S_{NO}^{S(10)} + S_{NH}^{S(10)} + S_{ND}^{S(10)} + X_{ND}^{S(10)} + i_{XB}(X_{BH}^{S(10)} + X_{BA}^{S(10)}) + i_{XP}(X_P^{S(10)} + X_I^{S(10)}), \quad (4c)$$

with stoichiometric parameters (f_P, i_{XB}, and i_{XP}) as per Gernaey et al. (2014). The effluent concentrations $X_a^{S(10)} = (X_{SS}^{S(10)}/X_f)X_a^{A(5)}$, for $a \in \{I, S, BH, BA, P, ND\}$, depend on $X_f = 0.75(X_I^{A(5)} + X_S^{A(5)} + X_{BH}^{A(5)} + X_{BA}^{A(5)} + X_P^{A(5)})$.

The state-space model for this class of ASPs is given as

$$\dot{x}(t) = f(x(t), u(t), w(t)|\theta_x); \quad (5a)$$

$$y(t) = g(x(t)|\theta_y), \quad (5b)$$

with state variables $x(t) = ((x^{A(1)}, \dots, x^{A(5)}), (x^{S(1)}, \dots, x^{S(10)}))^\mathsf{T} \in \mathbb{R}_{\geq 0}^{N_x}$, measurement variables $y(t) \in \mathbb{R}_{\geq 0}^{N_y}$, controllable inputs $u(t) = (Q_A, Q_R, Q_W, u^{A(1)}, \dots, u^{A(5)})^\mathsf{T} \in \mathbb{R}_{\geq 0}^{N_u}$, and disturbances $w(t) = (Q_{IN}, x^{A(IN)})^\mathsf{T} \in \mathbb{R}_{\geq 0}^{N_w}$, all at time t. The time-invariant dynamics $f(\cdot|\theta_x)$ and $g(\cdot|\theta_y)$ depend on a set of stoichiometric and kinetic parameters collectively denoted by the vectors θ_x and θ_y. The state-space model in Eq. (5) thus consists of $N_x = 13\times5+8\times10 = 145$ state variables, $N_u = 3+2\times5 = 13$ controls, $N_w = 1+13 = 14$ disturbances and $N_y = 5 \times 2 + 5 = 15$ outputs. As $N_x \gg N_u$ and $N_x \gg N_y$, the system is under-actuated and under-observed. We refer to Table 1 for a characterisation of the variables. The model in Eq. (5) is given in Appendix A.

The default control strategy proposed in Gernaey et al. (2014) for the BSM1 considers two low-level (PI) controllers:

- Nitrate and nitrite nitrogen in the second reactor, $S_{NO}^{A(2)}$, is controlled by manipulating the internal recycle, Q_A;
- Dissolved oxygen concentration in the fifth reactor, $S_O^{A(5)}$, is controlled by manipulating the oxygen mass transfer coefficient $K_L a^{(5)}$, a proxy to the air flow-rate.

The plant's performance is based on flow-weighted and time-averaged effluent concentrations of total suspended solids (X_{SS}), biochemical oxygen demand (BOD_5), chemical oxygen demand (COD), total nitrogen (N_{TOT}) and ammonia (S_{NH}). Typically, the control performance is given in terms of effluent quality by measuring and minimising the effluent concentration of these compounds (Gernaey et al., 2014).

Importantly, our state-space configuration includes all control handles suggested in Gernaey et al. (2014) that do not require changes to the plant layout depicted in Fig. 1. We consider the possibility of having the default low-level controllers applied on each of the five reactors. As such, our configuration necessarily includes a sensor-arrangement that considers the measurement of $S_{NO}^{A(r)}$ and $S_{O}^{A(r)}$ in all reactors ($r = 1, \dots, 5$).

3. Preliminaries: Dynamical properties and model decompositions

We consider the general state-space representation of a deterministic non-autonomous controlled dynamic system

$$\dot{x}(t) = f_t\big(x(t), u(t), w(t)|\theta_x\big) \tag{6a}$$

$$y(t) = g_t\big(x(t), u(t), w(t)|\theta_y\big) \tag{6b}$$

The state equation (6a), determines the evolution of the state $x(t) \in \mathbb{R}^{N_x}$, given its current value and a set of controllable and uncontrollable but measurable inputs $u(t) \in \mathbb{R}^{N_u}$ and $w(t) \in \mathbb{R}^{N_w}$. The measurement equation (6b) determines how the state is emitted as measurement $y(t) \in \mathbb{R}^{N_y}$. The nonlinear and time-varying functions $f_t(\cdot|\theta_x)$ and $g_t(\cdot|\theta_y)$ are fixed by the parameter vectors θ_x and θ_y. We consider autonomous functions $f(\cdot)$ and $g(\cdot)$, static state-feedback policies $u(t) = h(x(t)|\theta_u)$ with a fixed parameters θ_u, and no input feedthrough, $y(t) = g(x(t)|\theta_y)$. This allows to set $t_0 = 0$, though we often and intentionally omit mentioning it.

The structural form of the state-space representation of the system can be written using the usual linear model

$$\dot{x}(t) = Ax(t) + Bu(t) + Gw(t) \tag{7a}$$

$$y(t) = Cx(t) \tag{7b}$$

The structure of matrices A, B, G and C can be defined using inference diagrams in such a way that element $A_{n'_x,n_x}$ (respectively, B_{n_x,n_u}, G_{n_x,n_w} and C_{n_y,n_x}) is non-zero, and potentially unknown, whenever component x_{n_x} (u_{n_u}, w_{n_w} and again x_{n_x}) appears in the vector field $f_{n'_x}(\cdot)$ and algebraic function $g_{n_y}(\cdot)$; that is, whenever the (n'_x, n_x)-th element $\partial f_{n'_x}/\partial x_{n_x}$ (respectively, $\partial f_{n'_x}/\partial u_{n_u}$, $\partial f_{n'_x}/\partial w_{n_w}$ and $\partial g_{n_y}/\partial x_{n_x}$) in the Jacobian matrix(es) is non-zero. When the elements of A, B, G and C are either zeros or unknown, the resulting family of systems is referred to as structured dynamical system (Reinschke, 1988). Evaluating the Jacobians at a specific point (x', u', w') leads to an approximated linear time-invariant (LTI) system in which functions A, B, G and C are known. A steady-state point is usually chosen for fixing the linearisation.

Certain properties of structured and LTI systems can be studied by mapping the state equation Eq. (7a) onto the digraph

$$\mathcal{G}_c = (\mathcal{V}_c, \mathcal{E}_c), \tag{8}$$

where the vertex set $\mathcal{V}_c = \mathcal{V}_A \cup \mathcal{V}_B$ is the union of vertex set $\mathcal{V}_A = \{x_1, \dots, x_{N_x}\}$ of state components and vertex set $\mathcal{V}_B = \{u_1, \dots, u_{N_u}\}$ of controls, while the edge set $\mathcal{E}_c = \mathcal{E}_A \cup \mathcal{E}_B$ is the union of set $\mathcal{E}_A = \big\{(x_{n_x}, x_{n'_x}) \mid A_{n'_x,n_x} \neq 0\big\}$ of directed edges between state component vertices and set $\mathcal{E}_B = \big\{(u_{n_u}, x_{n_x}) \mid B_{n_x,n_u} \neq 0\big\}$ of directed edges between state and control vertices. The measurement process is studied by mapping the state and output equations Eq. (7) onto digraph

$$\mathcal{G}_o = (\mathcal{V}_o.\mathcal{E}_o), \tag{9}$$

Vertex set $\mathcal{V}_o = \mathcal{V}_A \cup \mathcal{V}_C$ is the union of vertex set $\mathcal{V}_A$ and vertex set $\mathcal{V}_C = \{y_1, \dots, y_{N_y}\}$ of outputs. Edge set $\mathcal{E}_o = \mathcal{E}_A \cup \mathcal{E}_C$ is the union of set $\mathcal{E}_A$ and set $\mathcal{E}_C = \big\{(x_{n_x}, y_{n_y}) \mid C_{n_y,n_x} \neq 0\big\}$ of directed edges between state and output vertices.

By coupling controls to state variables and state variables to measurements, the notions of controllability and observability define the prerequisite for control and state estimation. These conditions can be relaxed in the absence of unstable modes, in favour of the weaker notions of stabilisability and detectability. For linear systems, classical sufficient and necessary controllability and observability tests have been derived (Kalman, 1960). When a system is known only structurally, stronger notions of structural controllability and observability (Lin, 1974; Mayeda and Yamada, 1979) and associated sufficient and necessary conditions (Liu et al., 2011, 2013; Jarczyk et al., 2011; Jia et al., 2021) can be used. For LTI systems, the classical notions lead to important tools like the Kalman's canonical decomposition. For the sake of completeness and notational necessity, this section reviews all these concepts.

3.1. Stability

We review stability in terms of the conditions under which the system in Eq. (7) subjected to a bounded input produces bounded state- and output-response trajectories. These notions are referred to as external and internal stability, the latter one being more general. For simplicity and without any loss, we do not distignuish between controls and disturbances and momentarily redefine the control matrix to be $B \equiv [B|G]$.

A linear system with impulse response matrix $H(\cdot,\cdot) : \mathbb{R}_{\geq 0} \times \mathbb{R}_{\geq 0} \to \mathbb{R}^{N_y \times N_x}; (t, \tau) \mapsto H(t, \tau)$ is stable if $y(t) = \int_{t_0}^{t} H(t, \tau)u(\tau)\mathrm{d}\tau$ is bounded when $u(t)$ is bounded. This notion of external stability is defined as the existence of a finite gain $\kappa < \infty$ such that for all bounded inputs u the following relation holds $\|y(t)\|_\infty \leq \kappa \|u(t)\|_\infty$. External stability can be verified at the system level by showing that, under some mild conditions on the smoothness of u and H, the upper bound κ for the induced matrix norm of the input-output map exists and can be used as gain in aforementioned relation; that is,

$$\sup_{t \in \mathbb{R}_{\geq 0}} \left\{ \int_{t_0}^{t} \|H(t, \tau)\|_\infty \mathrm{d}\tau \right\} = \kappa < \infty. \tag{10}$$

For a LTI system, $H(t, \tau) = H(t - \tau) = Ce^{A(t-\tau)}B$. Condition Eq. (10) specialises and it suffices to show that *i*) the impulse response is absolutely integrable and *ii*) the transfer

function $H(s) = \mathcal{L}[H(t)] = C(sI - A)^{-1}B$ is Hurwitz:

$$i) \quad \int_{t_0}^{\infty} \|H(t)\| \mathrm{d}t < \infty; \tag{11a}$$

$$ii) \quad \{\lambda[H(s)] \in \mathbb{C} : \mathtt{Re}(\lambda) < 0\}. \tag{11b}$$

More generally, system (A, B, C) with state transition matrix $\Phi(\cdot,\cdot) : \mathbb{R}_{\geq 0} \times \mathbb{R}_{\geq 0} \to \mathbb{R}^{N_x \times N_x}; (t, \tau) \mapsto \Phi(t, \tau)$ is stable if both $x(t) = \Phi(t, t_0)x(t_0) + \int_{t_o}^{t} \Phi(t, \tau)Bu(\tau)\mathrm{d}\tau$ and $y(t) = C\Phi(t, t_0)x(t_0) + C\int_{t_o}^{t} \Phi(t, \tau)Bu(\tau)\mathrm{d}\tau$ are bounded for every bounded $u(t)$. This notion of joint internal and external stability is defined for representations with bounded functions B and C (i.e., when $\|B\|_\infty < \infty$ and $\|C\|_\infty < \infty$) as the existence of positive constants β and γ such that Eqs. (12) hold for every bounded input u and initial condition x_0:

$$\|x(t)\|_\infty \leq \beta\|x_0\| + \left((\beta/\gamma)\|B\|_\infty\right)\|u(t)\|_\infty \tag{12a}$$

$$\|y(t)\|_\infty \leq \left(\beta\|C\|_\infty\right)\|x_0\| + \left((\beta/\gamma)\|C\|_\infty\|B\|_\infty\right)\|u(t)\|_\infty \tag{12b}$$

The definition is valid only for systems whose homogeneous part is exponentially stable with the same constants β and γ (when $\|\Phi(t, \tau)\| \leq \beta e^{-\gamma(t-\tau)}$). Internal and external stability in Eqs. (12) are verified by showing that matrix A is Hurwitz:

$$\{\lambda[A] \in \mathbb{C} : \mathrm{Re}(\lambda) < 0\}. \tag{13}$$

For the LTI system in Eq. (7) where $\Phi(t, \tau) = e^{A(t-\tau)}$, the entries of the state transition matrix are linear combinations of the system modes. By letting $\lambda[A] = \{\lambda_{n_x}\}_{n_x=1}^{N_x}$ denote the eigenvalues of A, with $\{\lambda_1, \ldots, \lambda_N\} \subseteq \mathbb{R}$ and $\{(\lambda_{N+1}, \lambda^*_{N+1}), \ldots, (\lambda_{N+S}, \lambda^*_{N+S})\} \subseteq \mathbb{C}$ being the eigenvalues with respective algebraic multiplicities $\mu(\lambda_{n_x})$, and given $\alpha^{(i,j)}_{n,k}, \beta^{(i,j)}_{n,k}, \phi^{(i,j)}_{n,k} \in \mathbb{R}$, each (i, j)-th entry in e^{At} is of the form

$$[e^{At}]_{i,j} = \sum_{n=1}^{N} \sum_{k=0}^{\mu(\lambda_n)-1} (\alpha^{(i,j)}_{n,k} t^k) e^{\lambda_n t} + \sum_{n=N+1}^{N+S} \sum_{k=0}^{\mu(\lambda_n)-1} (\beta^{(i,j)}_{n,k} t^k \cos\left(\mathtt{Im}(\lambda_n)t + \phi^{(i,j)}_{n,k}\right)) e^{\mathrm{Re}(\lambda_n)t}. \tag{14}$$

The condition Eq. (13) implies that $\lim_{t\to\infty} [\Phi(t, \tau)]_{i,j} = 0$, for all (i, j). Therefore, it is possible to verify exponential stability at the system level since that, for any fixed $\tau \leq t$, the homogeneous part is strictly decreasing with $\max_t \|\Phi(t, \tau)\| = \|\Phi(\tau, \tau)\| \leq \beta$ and $\lim_{t\to\infty} \|\Phi(t, \tau)\| = 0$.

3.2. Controllability and observability

A system is full-state controllable if it is possible to steer it from any initial state to any final state in finite time, whereas it is full-state observable if it is possible to uniquely determine its initial state from a sequence of measurements over a finite time. These notions are overviewed and classical necessary and sufficient conditions are given for LTI systems. For systems that are controllable and observable, we review a set of energy-based controllability and observability metrics. We also review the more general structural notions of these notions and provide weak and strong validity conditions.

3.2.1. Classical controllability and observability

Let the controllability Gramian of the pair (A, B) be the $N_x \times N_x$ symmetric positive semidefinite matrix

$$W_c(t) = \int_0^t e^{A\tau} BB^{\mathsf{T}} e^{A^{\mathsf{T}}\tau} \mathrm{d}\tau. \tag{15}$$

A sufficient and necessary controllability condition is

$$\mathtt{det}\big(W_c(t)\big) \neq 0, \quad \forall t > 0. \tag{16}$$

Let the observability Gramian of the pair (A, C) be the $N_x \times N_x$ symmetric positive semidefinite matrix

$$W_o(t) = \int_0^t e^{A^{\mathsf{T}}\tau} C^{\mathsf{T}} C e^{A\tau} \mathrm{d}\tau. \tag{17}$$

A sufficient and necessary observability condition is

$$\mathtt{det}\big(W_o(t)\big) \neq 0, \quad \forall t > 0. \tag{18}$$

Gramian-based criteria in Eqs. (16) and (18) are straightforward but unpractical. Equivalent criteria can be defined from controllability and observability matrices (Kalman, 1960).

Let $\mathcal{C} = \begin{bmatrix} B & AB & A^2B & \cdots & A^{N_x-1}B \end{bmatrix}$ be the $N_x \times (N_x \times N_u)$ controllability matrix of the system. Let $\mathcal{O} = \begin{bmatrix} C^{\mathsf{T}} & A^{\mathsf{T}}C^{\mathsf{T}} & (A^{\mathsf{T}})^2C^{\mathsf{T}} & \cdots & (A^{\mathsf{T}})^{N_x-1}C^{\mathsf{T}} \end{bmatrix}^{\mathsf{T}}$ be the $(N_y \times N_x) \times N_x$ observability matrix of the system. Sufficient and necessary condition for controllability and observability are

$$\mathtt{rank}(\mathcal{C}) = N_x; \tag{19a}$$

$$\mathtt{rank}(\mathcal{O}) = N_x. \tag{19b}$$

The criteria in Eqs. (19a) and Eq. (19b) are more direct and, for low-dimensional systems, their evaluation only requires a small number of matrix multiplications. The computation of $\mathcal{C}$ and $\mathcal{O}$ can still be troublesome for high-dimensional systems. The limitation is due to numerical over- and underflows resulting from computing large powers of A and A^{T}. A scalable alternative that overcomes the limitations of both Gramian-based and Kalman's rank criteria is provided by the Popov-Belevitch-Hautus (PBH) rank tests. Necessary and sufficient conditions are given by the two following lemmas:

Lemma 1. *(Hautus, 1970). The statement 'the pair* (A, B) *is controllable' is equivalent to the statements:*

$$\mathtt{rank}(\begin{bmatrix} \lambda I - A & B \end{bmatrix}) = N_x, \ \forall \lambda \in \mathbb{C}; \tag{20a}$$

$$\mathtt{rank}(\begin{bmatrix} \lambda_i I - A & B \end{bmatrix}) = N_x, \ \forall \lambda_i \in \sigma(A) \subset \mathbb{C}. \tag{20b}$$

Lemma 2. *(Hautus, 1970). The statement 'the pair* (A, C) *is observable' is equivalent to the statements:*

$$\mathtt{rank}(\begin{bmatrix} \lambda I - A^{\mathsf{T}} & C^{\mathsf{T}} \end{bmatrix}^{\mathsf{T}}) = N_x, \ \forall \lambda \in \mathbb{C}; \tag{21a}$$

$$\mathtt{rank}(\begin{bmatrix} \lambda_i I - A^{\mathsf{T}} & C^{\mathsf{T}} \end{bmatrix}^{\mathsf{T}}) = N_x, \ \forall \lambda_i \in \sigma(A) \subset \mathbb{C}. \tag{21b}$$

Based on Lemma 1, the pair (A, B) is controllable if and only if, for each eigenvalue $\lambda_i \in \sigma(A)$ (that is, when $\mathtt{rank}(\lambda_i I -$

$A) < N_x$), the columns of $\boldsymbol{B}$ have at least one component in the direction $\nu_i \in \mathbb{R}^{N_x}$, being ν_i the eigenvector of A associated to λ_i; The eigenvectors ν_i for which $\mathtt{rank}([\lambda_i I - A\ B]) < N_x$ are state-space directions that are uncontrollable with the controls determined by $\boldsymbol{B}$. Based on Lemma 2, the pair (A, C) is observable if and only if, for each $\lambda_i \in \sigma(A)$ (that is, when $\mathtt{rank}(\lambda_i I - A^{\mathsf{T}}) < N_x$), the columns of $\boldsymbol{C}$ have at least one component in the direction $\nu_i \in \mathbb{R}^{N_x}$, being ν_i the eigenvector of A associated to λ_i; The eigenvectors ν_i for which $\mathtt{rank}([\lambda_i I - A^{\mathsf{T}}\ C^{\mathsf{T}}]^{\mathsf{T}}) < N_x$ are directions that are unobservable with the measurements determined by $\boldsymbol{C}$.

Controllability and observability are invariant with respect to nonsingular similarity transformations $P \in \mathbb{R}^{N_x \times N_x}$. Thus,

- the pair (A, B) is controllable if and only if the pair $(A', B') = (P^{-1}AP, P^{-1}B)$ is controllable;
- the pair (A, C) is observable if and only if the pair $(A', C') = (P^{-1}AP, CP)$ is observable.

Controllability and observability metrics

Full-state controllability and observability are binary properties. Starting from the seminal work by Müller and Weber (1972), various scalar metrics have been proposed to quantify the difficulty of control and observation tasks. We overview some energy-related metrics recently proposed by Pasqualetti et al. (2014), and Summers et al. (2016) for LTI systems.

Define the quadratic control and measurement energies

$$E_c(u(t), t|R) = \int_0^t u(\tau)^{\mathsf{T}} R u(\tau) \mathrm{d}\tau = \|u(t)\|^2_{2|R}; \tag{22a}$$

$$E_o(y(t), t|Q) = \int_0^t y(\tau)^{\mathsf{T}} Q y(\tau) \mathrm{d}\tau = \|y(t)\|^2_{2|Q}. \tag{22b}$$

In optimal quadratic regulation, we search for a controller that minimises these energies given positive definite weighting matrices $R \in \mathbb{R}^{N_x \times N_x}$ and $Q \in \mathbb{R}^{N_y \times N_y}$. When minimised with $R = I_u$ and $Q = I_y$, the unweighted energies determine

- $\tilde{u}(t) = B^{\mathsf{T}} e^{A^{\mathsf{T}}(t)} W_c^{-1}(t)(x(t) - e^{At}x(0))$, the control from $x(0)$ to $x(t)$ of minimum L_2-effort

$$E_c^*(t|\tilde{u}(t)) = (x(t) - e^{At}x(0))^{\mathsf{T}} W_c^{-1}(t)\big(x(t) - e^{At}x(0)\big);$$

- $x(0) = W_o^{-1}(t) \int_0^t e^{A^{\mathsf{T}}\tau} C^{\mathsf{T}} y(\tau) \mathrm{d}\tau$, the initial state from measurement $\tilde{y}(t)$ of minimum L_2-effort

$$E_o^*(t|\tilde{y}(t)) = x(0)^{\mathsf{T}} W_o(t) x(0).$$

Finite- and infinite-horizon controllability and observability metrics can be derived from Eq. (16) and (18). The eigenvectors $\left\{\nu_{n_x}(\lambda^c_{n_x})\right\}_{n_x=1}^{N_x}$ associated with the eigenvalues $\lambda^c_{n_x} \in \sigma\big(W_c(t)\big)$ correspond to state-space directions that require increasingly larger control energy the smaller $\lambda^c_{n_x}$, whereas the eigenvectors $\left\{\nu_{n_x}(\lambda^o_{n_x})\right\}_{n_x=1}^{N_x}$ associated with the eigenvalues $\lambda^o_{n_x} \in \sigma\big(W_o(t)\big)$ correspond to directions of increasingly larger output energy the larger $\lambda^o_{n_x}$. The control and measurement efforts associated with pairs (A, B) and (A, C) can thus be quantified by single scalars defined from spectra $\sigma\big(W_c(t)\big) = \left\{\lambda^c_{n_x}\right\}_{n_x=1}^{N_x}$ and $\sigma\big(W_o(t)\big) = \left\{\lambda^o_{n_x}\right\}_{n_x=1}^{N_x}$.

Infinite-time Gramians, $W_c(\infty)$ and $W_o(\infty)$, always exist for Hurwitz systems, Eq. (13), and can be efficiently computed by solving Lyapunov equations (Benner et al., 2008). Thus, we only review a number of infinite-time metrics: Finite-time counterparts are evaluated by integrating Eqs. (16) and (18).

Definition 1. (Energy-related controllability metrics) Let $W_c(\infty)$ be the solution of $AW_c(\infty) + W_c(\infty)A^{\mathsf{T}} + BB^{\mathsf{T}} = 0$. The control effort for (A, B) is quantified by the scalars:

I. $\mathtt{trace}\left(W_c(\infty)\right)$: It is inversely related to the control effort averaged over all state-space directions;
II. $\mathtt{trace}\left(W_c^{\dagger}(\infty)\right)$: It is related to the control effort averaged over all directions in the state-space;
III. $\log\left(\mathtt{det}(W_c(\infty))\right)$: It is related to the volume of a N_x-dimensional hyper-ellipsoid whose points are reachable with one unit or less of control energy;
IV. $\lambda^c_{\min}\left(W_c(\infty)\right)$: It is inversely related to the control energy along the least controllable eigen-direction.

Definition 2. (Energy-related observability metrics) Let $W_o(\infty)$ be the solution of $W_o(\infty)A^{\mathsf{T}} + AW_o(\infty) + C^{\mathsf{T}}C = 0$. The output effort for (A, C) is quantified by the scalars:

I. $\mathtt{trace}\left(W_o(\infty)\right)$: It is inversely related to the output effort averaged over all state-space directions;
II. $\mathtt{trace}\left(W_o^{\dagger}(\infty)\right)$: It is related to the output effort averaged over all directions in the state-space;
III. $\log\left(\mathtt{det}(W_o(\infty))\right)$: It is related to the volume of a N_x-dimensional hyper-ellipsoid whose points are observable with one unit or less of output energy;
IV. $\lambda^o_{\min}\left(W_o(\infty)\right)$: It is inversely related to the output energy along the least observable eigen-direction.

The control effort associated with attempting to control the full-state by only controlling one individual state variable x_{n_x} at a time is quantified by the average controllability centrality

$$C_c(n_x) = \mathtt{trace}\big(W_{c,n_x}(\infty)\big). \tag{23}$$

This non-negative quantity is computed when a single control acts only on the n_x-th state variable, when $\boldsymbol{B} = e_{n_x}$ is a unit vector in the standard basis of $\mathbb{R}^{N_x}$. Infinite-horizon Gramians $W_{c,n_x}(\infty) \in \mathbb{R}^{N_x \times N_x}$ solve the Lyapunov equations $AW_{c,n_x}(\infty) + W_{c,n_x}(\infty)A^{\mathsf{T}} = -e_{n_x}e_{n_x}^{\mathsf{T}}$ for $n_x \in \{1, \dots, N_x\}$.

The measurement effort associated with attempting to reconstruct the full-state by only measuring one state variable x_{n_x} at a time is quantified by the average observability centrality

$$C_o(n_x) = \mathtt{trace}\big(W_{o,n_x}(\infty)\big). \tag{24}$$

This non-negative quantity is computed when a single sensor measures directly only the n_x-th state variable, when $C = e_{n_x}^\top$ is a unit vector in $\mathbb{R}^{N_x}$. The infinite-horizon Gramians $W_{o,n_x}(\infty) \in \mathbb{R}^{N_x \times N_x}$ are computed for all $n_x \in \{1, \dots, N_x\}$ as solutions to $W_{o,n_x}(\infty)A^\top + AW_{o,n_x}(\infty) = -e_{n_x} e_{n_x}^\top$.

3.2.2. Structural controllability and observability

Structural analysis aims at assessing a family of systems with the same structure. The dynamics and measurement process of a structured dynamical system (A, B, C) can be studied by mapping its state and output equations onto the digraph

$$\mathcal{G} = (\mathcal{V}, \mathcal{E}), \tag{25}$$

where the vertex set $\mathcal{V} = \mathcal{V}_A \cup \mathcal{V}_B \cup \mathcal{V}_C$ consists of the union of vertex sets $\mathcal{V}_A = \{x_1, \dots, x_{N_x}\}$ of state, $\mathcal{V}_B = \{u_1, \dots, u_{N_u}\}$ of control, and $\mathcal{V}_C = \{y_1, \dots, y_{N_y}\}$ of output components. The edge set $\mathcal{E} = \mathcal{E}_A \cup \mathcal{E}_B \cup \mathcal{E}_C$ is the union of set $\mathcal{E}_A = \{(x_{n_x}, x_{n'_x}) \mid A_{n'_x,n_x} \neq 0\}$ of directed edges between state component vertices, set $\mathcal{E}_B = \{(u_{n_u}, x_{n_x}) \mid B_{n_x,n_u} \neq 0\}$ of directed edges between state and control component vertices, and set $\mathcal{E}_C = \{(x_{n_x}, y_{n_y}) \mid C_{n_y,n_x} \neq 0\}$ of directed edges between state and output component vertices.

The structural controllability of the family of systems with dynamics represented by pair (A, B) can be studied through its associated directed subgraph $\mathcal{G}_c = (\mathcal{V}_c, \mathcal{E}_c)$, defined by vertex set $\mathcal{V}_c = \mathcal{V}_A \cup \mathcal{V}_B$ and edge set $\mathcal{E}_c = \mathcal{E}_A \cup \mathcal{E}_B$. By duality, the structural observability of the family of systems with measurement process represented by (A, C) can be studied through its associated directed subgraph $\mathcal{G}_o = (\mathcal{V}_o, \mathcal{E}_o)$, defined by vertex set $\mathcal{V}_o = \mathcal{V}_A \cup \mathcal{V}_C$ and edge set $\mathcal{E}_o = \mathcal{E}_A \cup \mathcal{E}_C$.

The pair (A, B) is structurally controllable if the nonzero elements of A and B can be set in such a way that the system is controllable in the classical sense. Pair (A, C) is structurally observable if the nonzeros of A and C can be set in such a way that the system is observable in the classical sense. Formally, for an arbitrarily small $\varepsilon > 0$, we have the definitions

Definition 3. (Structural controllability, (Lin, 1974)). The pair (A, B) is structurally controllable if and only if there exists a controllable pair $(\bar{A}, \bar{B})$ of the same dimension and structure of (A, B) such that $\|\bar{A} - A\| < \varepsilon$ and $\|\bar{B} - B\| < \varepsilon$.

Definition 4. (Structural observability, (Lin, 1974)). The pair (A, C) is structurally observable if and only if there exists an observable pair $(\bar{A}, \bar{C})$ of the same dimension and structure of (A, C) such that $\|\bar{A} - A\| < \varepsilon$ and $\|\bar{C} - C\| < \varepsilon$.

Two pairs (A, B) and $(\bar{A}, \bar{B})$ have the same structure if they have the same dimensions and each element $A_{n'_x,n_x} \neq 0$ (respectively, $B_{n_x,n_u} \neq 0$) whenever $\bar{A}_{n'_x,n_x} \neq 0$ (respectively, $\bar{B}_{n_x,n_u} \neq 0$). The same applies for pairs (A, C) and $(\bar{A}, \bar{C})$. Necessary and sufficient conditions for structural controllability and observability can be derived from (Lin, 1974):

Lemma 3. *Let $\mathcal{G}_c = (\mathcal{V}_c, \mathcal{E}_c)$ be the network associated to the pair (A, B). The pair (A, B) is said to be structurally controllable if and only if the following conditions hold:*

- *(Accessibility) For every $x_{n_x} \in \mathcal{V}_A$ there exists at least one directed path from any $u_{n_u} \in \mathcal{V}_B$ to x_{n_x}.*
- *(Dilation-free) For every $\mathcal{S} \subseteq \mathcal{V}_A$, $|T(\mathcal{S})| \geq |\mathcal{S}|$, where $T(\mathcal{S}) = \{v_j \in \mathcal{V}_c \mid x_{n_x} \in \mathcal{S} \wedge (v_j, x_{n_x}) \in \mathcal{E}_c\}$ denotes a neighbourhood set for $\mathcal{S}$.*

Lemma 4. *Let $\mathcal{G}_o = (\mathcal{V}_o, \mathcal{E}_o)$ be the network associated to the pair (A, C). The pair (A, C) is said to be structurally observable if and only if the following conditions hold:*

- *(Accessibility) For every $x_{n_x} \in \mathcal{V}_A$ there exists at least one directed path from x_{n_x} to any $y_{n_y} \in \mathcal{V}_C$.*
- *(Dilation-free) For every $\mathcal{S} \subseteq \mathcal{V}_A$, $|T(\mathcal{S})| \geq |\mathcal{S}|$, where $T(\mathcal{S}) = \{v_j \in \mathcal{V}_o \mid x_{n_x} \in \mathcal{S} \wedge (x_{n_x}, v_j) \in \mathcal{E}_o\}$ denotes a neighbourhood set for $\mathcal{S}$.*

The first condition in Lemma 3 can be verified by identifying the state vertices that are accessible from each possible origin vertex (a control). Similarly, the first condition in Lemma 4 can be verified by identifying the output vertices that are accessible from each possible origin vertex (a state component). Any graph search algorithm can be used for both tasks (Cormen et al., 2009). The second condition in both lemmas can be verified by forming a maximum matching $\mathcal{M} \subseteq \Gamma$ of an equivalent bipartite graph $\mathcal{K} = (\mathcal{V}_A^+, \mathcal{V}_A^-, \Gamma)$, then checking that all unmatched state vertices $x_j \in \mathcal{V}_A^-$ are directly connected to distinct control vertices in $\mathcal{G}_c = (\mathcal{V}_c, \mathcal{E}_c)$, in case of Lemma 3, or are directly connected to distinct output vertices in $\mathcal{G}_o = (\mathcal{V}_o, \mathcal{E}_o)$ in case of Lemma 4 (Liu et al., 2011).

The maximum matching problem consists of identifying a (possibly not unique) subset of edges without common vertices that has maximum cardinality. The bipartite graph $\mathcal{K} = (\mathcal{V}_A^+, \mathcal{V}_A^-, \Gamma)$ is defined by the disjoint and independent vertex sets $\mathcal{V}_A^+ = \{x_1^+, \dots, x_{N_x}^+\}$ and $\mathcal{V}_A^- = \{x_1^-, \dots, x_{N_x}^-\}$, and by the undirected edge set $\Gamma = \{(x_{n'_x}^+, x_{n_x}^-) \mid (x_{n'_x}, x_{n_x}) \in \mathcal{E}_A\}$. Unmatched state vertices linked to distinct control or output vertices form a $\mathcal{V}_A^-$−perfect matching. The dilation-free condition is guaranteed from the Hall's theorem (Hall, 1935).

Strong controllability and observability

Based on Lin (1974), a structurally controllable (respectively, structural observable) system might, under certain conditions, still admit full-state uncontrollable (respectively, full-state unobservable) realisations (Zhao et al., 2015). This limitation can be overcome with the notions of strong structural controllability and observability (Mayeda and Yamada, 1979).

A structural pair (A, B) is strongly controllable in a structural sense if every possible realisation of its nonzero entries leads to a full-state controllable system. By duality, a structural pair (A, C) is strongly observable in a structural sense

if every possible realisation of its nonzero entries leads to a full-state observable system. A strongly structurally controllable (respectively, observable) system is always structurally controllable (observable), the converse is not always true:

Definition 5. (Strong structural controllability, (Mayeda and Yamada, 1979)) The pair (A, B) is strongly structurally controllable if and only if any pair $(\bar{A}, \bar{B})$ of the same dimension and structure of (A, B) is controllable in the classical sense.

Definition 6. (Strong structural observability, (Mayeda and Yamada, 1979)) The pair (A, C) is strongly structurally observable if and only if any pair $(\bar{A}, \bar{C})$ of the same dimension and structure of (A, C) is observable in the classical sense.

Sufficient and necessary conditions for strong structural controllability of (A, B) can be derived from its associated network $\mathcal{G}_c = (\mathcal{V}_c, \mathcal{E}_c)$ and a digraph $\widetilde{\mathcal{G}}_c = (\mathcal{V}_c, \widetilde{\mathcal{E}}_c)$, in which

$$\widetilde{\mathcal{E}}_c = \left\{(x_{n_x}, x_{n'_x}) \mid A_{n'_x,n_x} \neq 0,\ n'_x \neq n_x\right\} \cup \left\{(x_{n_x}, x_{n_x}) \mid A_{n_x,n_x} = 0\right\} \cup \mathcal{E}_B. \quad (26)$$

The conditions for strong structural observability of (A, C) result from $\mathcal{G}_o = (\mathcal{V}_o, \mathcal{E}_o)$ and a digraph $\widetilde{\mathcal{G}}_o = (\mathcal{V}_o, \widetilde{\mathcal{E}}_o)$ where

$$\widetilde{\mathcal{E}}_o = \left\{(x_{n_x}, x_{n'_x}) \mid A_{n'_x,n_x} \neq 0,\ n'_x \neq n_x\right\} \cup \left\{(x_{n_x}, x_{n_x}) \mid A_{n_x,n_x} = 0\right\} \cup \mathcal{E}_C. \quad (27)$$

Lemma 5. *(Jia et al., 2021) Let $\mathcal{G}_c = (\mathcal{V}_c, \mathcal{E}_c)$ be the network associated to the pair (A, B) and $\widetilde{\mathcal{G}}_c = (\mathcal{V}_c, \widetilde{\mathcal{E}}_c)$ an alternative graph with edge set $\widetilde{\mathcal{E}}_c$ defined by Eq. (26). The pair (A, B) is said to be strongly structurally controllable if and only if both $\mathcal{G}_c = (\mathcal{V}_c, \mathcal{E}_c)$ and $\widetilde{\mathcal{G}}_c = (\mathcal{V}_c, \widetilde{\mathcal{E}}_c)$ are colourable.*

Lemma 6. *(Jia et al., 2021) Let $\mathcal{G}_o = (\mathcal{V}_o, \mathcal{E}_o)$ be the network associated to the pair (A, C) and $\widetilde{\mathcal{G}}_o = (\mathcal{V}_o, \widetilde{\mathcal{E}}_o)$ an alternative graph with edge set $\widetilde{\mathcal{E}}_o$ defined by Eq. (27). The pair (A, C) is said to be strongly structurally observable if and only if both $\mathcal{G}_o = (\mathcal{V}_o, \mathcal{E}_o)$ and $\widetilde{\mathcal{G}}_o = (\mathcal{V}_o, \widetilde{\mathcal{E}}_o)$ are colourable.*

The graph colouring procedure is described as follows:

1) Initially, colour all vertices $v_c \in \mathcal{V}_c$ white;
2) Colour v_j black if $(v_i, v_j) \in \mathcal{E}_c$ and $(v_i, v_k) \notin \mathcal{E}_c$ for a fixed $v_i \in \mathcal{V}_c$ and for all $v_j, v_k \in \mathcal{V}_c$ with $v_j \neq v_k$;
3) Repeat step 2 until no more colour changes are possible.

This procedure is similarly defined for graphs $\widetilde{\mathcal{G}}_o = (\mathcal{V}_o, \widetilde{\mathcal{E}}_o)$ and $\widetilde{\mathcal{G}}_o = (\mathcal{V}_o, \widetilde{\mathcal{E}}_o)$. A graph is denoted colourable if all nodes $x_{n_x} \in \mathcal{V}_A$ are coloured black according to this procedure.

Controllability and observability centralities

The relevance of a node in a graph is quantified by its centrality (Estrada and Knight, 2015). We overview the centrality of individual state variables as encoded by the subgraph $\mathcal{G}_A = (\mathcal{V}_A, \mathcal{E}_A)$ of state nodes and their mutual relations. We look at node centralities as basic structural equivalent of control and observation energy-based metrics (Bof et al., 2017).

The in-degree centrality of state node x_{n_x} is defined as

$$k_{in}(n_x) = [A\mathbf{1}]_{n_x}, \quad (28)$$

where $\mathbf{1}$ is a N_x-th dimensional vector of all ones. $k_{in}(n_x)$ counts incoming edges to node x_{n_x}, the number of state variables that directly affect its dynamics. For observability, $k_{in}(n_x)$ quantifies how many state variables are indirectly observed if we were to measure only the n_x-th state variable.

The out-degree centrality of state node x_{n_x} is defined as

$$k_{out}(n_x) = \left[A^{\mathsf{T}}\mathbf{1}\right]_{n_x}. \quad (29)$$

$k_{out}(n_x)$ counts the outgoing edges from node x_{n_x}, the number of state-variables whose dynamics are directly affected by the n_x-th state variable. For controllability, $k_{out}(n_x)$ measures the number of state variables whose evolution is indirectly affected if we were to control only the n_x-th state variable.

3.3. Reduced-order models

A non-controllable (respectively, non-observable) system can be decomposed into controllable and non-controllable (observable and non-observable) parts by a similarity transformation $P_c \in \mathbb{R}^{N_x \times N_x}$ ($P_o \in \mathbb{R}^{N_x \times N_x}$). We review the Kalman decomposition theorem for obtaining minimal realisations of LTI systems from such transformations. For non-controllable and non-observable systems, the weaker properties of stabilisability and detectability are also overviewed.

3.3.1. Kalman decomposition theorem

Let $S \in \mathbb{R}^{N_{\tilde{x}} \times N_x}$ and $T \in \mathbb{R}^{N_x \times N_{\tilde{x}}}$ be a pair of transformation matrices satisfying $ST = I$. The linear transformation $\tilde{x} = Sx$ resulting in the state-space representation

$$\dot{\tilde{x}}(t) = \widetilde{A}\tilde{x}(t) + \widetilde{B}u(t)$$
$$y(t) = \widetilde{C}\tilde{x}(t),$$

with $\widetilde{A} \in \mathbb{R}^{N_{\tilde{x}} \times N_{\tilde{x}}} = SAT$, $\widetilde{B} \in \mathbb{R}^{N_{\tilde{x}} \times N_u} = SB$, and $\widetilde{C} \in \mathbb{R}^{N_y \times N_{\tilde{x}}} = CT$, is a $N_{\tilde{x}}$-order reduced model of the full-order model (A, B, C) whenever $N_{\tilde{x}} < N_x$. The quality of $(\widetilde{A}, \widetilde{B}, \widetilde{C})$ can be quantified by the approximation error

$$\|\widetilde{G} - G\|_{\mathcal{H}_\infty} \|u\|_{\mathcal{L}_2} \quad (\forall u \in \mathbb{R}^{N_u}),$$

for $\widetilde{G}(s) = \widetilde{C}(sI - \widetilde{A})^{-1}\widetilde{B}$ and $G(s) = C(sI - A)^{-1}B$.

A perfect reduced-order model is the minimal realisation of (A, B, C) computed by the Kalman decomposition theorem:

Lemma 7. *(Minimal Realisation, Kalman (1963)). Let $\mathcal{C}$ and $\mathcal{O}$ be, respectively, the controllability and observability matrix of a full-order model (A, B, C), with $\mathrm{rank}(\mathcal{C}) = N_C$, $\mathrm{rank}(\mathcal{O}) = N_{\mathcal{O}}$ and $\mathrm{rank}([\mathcal{C}\ \mathcal{O}^{\mathsf{T}}]) = N_{C\mathcal{O}}$. Now, let*

$\tilde{x} = [x_{co}\ x_{\bar{c}o}\ x_{c\bar{o}}\ x_{\bar{c}\bar{o}}]^\mathsf{T} = P^{-1}x$ be a linear transformation converting (A, B, C) into Kalman's canonical form

$$\begin{bmatrix}\dot{x}_{co}(t)\\ \dot{x}_{c\bar{o}}(t)\\ \dot{x}_{\bar{c}o}(t)\\ \dot{x}_{\bar{c}\bar{o}}(t)\end{bmatrix} = \begin{bmatrix}A_{co} & 0 & A_{13} & 0\\ A_{21} & A_{c\bar{o}} & A_{23} & A_{24}\\ 0 & 0 & A_{\bar{c}o} & 0\\ 0 & 0 & A_{43} & A_{\bar{c}\bar{o}}\end{bmatrix}\begin{bmatrix}x_{co}(t)\\ x_{c\bar{o}}(t)\\ x_{\bar{c}o}(t)\\ x_{\bar{c}\bar{o}}(t)\end{bmatrix} + \begin{bmatrix}B_{co}\\ B_{c\bar{o}}\\ 0\\ 0\end{bmatrix}u(t)$$
$$y(t) = \begin{bmatrix}C_{co} & 0 & C_{\bar{c}o} & 0\end{bmatrix}\tilde{x}(t).$$

The minimal realisation (A_{co}, B_{co}, C_{co}) is a reduced model of order $N_{x_{co}} = N_C + N_{\mathcal{O}} - N_{C\mathcal{O}}$.

The minimal realisation is a reduced model which is both controllable and observable. Minimal realisations can be computed efficiently, as the computation of $\mathcal{C}$ and $\mathcal{O}$ can be avoided (Van Dooren, 1981). Moreover, $\widetilde{G}(s) = C_{co}(sI - A_{co})^{-1}B_{co} = C(sI-A)^{-1}B = G(s)$, such that this realisation is a perfect approximation with error $\|\widetilde{G} - G\|_{\mathcal{H}_\infty}\|u\|_{\mathcal{L}_2} = 0$, for all $u \in \mathbb{R}^{N_u}$. A minimal realisation has full-order $N_{x_{co}} = N_x$ whenever (A, B, C) is both controllable and observable.

3.3.2. Stabilisability and detectability

A system is stabilisable if it possible to steer it from any initial state to the zero-state (a steady-state, for linearised systems), whereas it is detectable if its initial state can be asymptotically approximated from a sequence of measurements. Formally,

Definition 7. (Stabilizability). The pair (A, B) is said to be stabilisable if, given any initial state $x(0)$, it is possible to design an input $u(t)$ such that $x(t) \to 0$ as $t \to \infty$.

Definition 8. (Detectability). The pair (A, C) is said to be detectable if, giving any initial state $x(0)$, it is possible to compute a state estimate $\hat{x}(t)$ from the force-free evolution of $y(t)$, so that $(x(t) - \hat{x}(t)) \to 0$ as $t \to \infty$.

Sufficient and necessary conditions for stabilisability and detectability can be derived from a Kalman canonical decomposition. Let $\mathcal{C} = [B\ AB\ A^2B\ \cdots\ A^{N_x-1}B]$ be the $\mathbb{R}^{N_x \times N_x N_u}$ controllability matrix of (A, B), with $\mathtt{rank}(\mathcal{C}) = N_{x_c} \leq N_x$. There exists a nonsingular matrix $P_c \in \mathbb{R}^{N_x \times N_x}$, whose first N_{x_c} columns are the linearly independent columns of $\mathcal{C}$, such that the transformation $x_c = P_c^{-1}x$ has a state equation

$$\begin{bmatrix}\dot{x}_c(t)\\ \dot{x}_{\bar{c}}(t)\end{bmatrix} = \begin{bmatrix}A_c & A_{12}\\ 0 & A_{\bar{c}}\end{bmatrix}\begin{bmatrix}x_c(t)\\ x_{\bar{c}}(t)\end{bmatrix} + \begin{bmatrix}B_c\\ 0\end{bmatrix}u(t),$$

with $x_c(t) \in \mathbb{R}^{N_{x_c}}$ and $x_{\bar{c}}(t) \in \mathbb{R}^{(N_x - N_{x_c})}$. A sufficient and necessary condition for stabilizability is that $\mathtt{Re}(\lambda_j) < 0$ for all $\lambda_j \in \sigma(A_{\bar{c}}) \subset \sigma(A)$ (Callier and Desoer, 1991). Similarly, let $\mathcal{O} = [C^\mathsf{T}\ A^\mathsf{T}C^\mathsf{T}\ (A^\mathsf{T})^2C^\mathsf{T}\ \cdots\ (A^\mathsf{T})^{N_x-1}C^\mathsf{T}]^\mathsf{T}$ be the $\mathbb{R}^{N_y N_x \times N_x}$ observability matrix of (A, C), with $\mathtt{rank}(\mathcal{O}) = N_{x_o} \leq N_x$. There exists a nonsingular matrix $P_o \in \mathbb{R}^{N_x \times N_x}$, whose first N_{x_o} rows are the linearly independent rows of $\mathcal{O}$, such that transformation $x_o = P_o^{-1}x$ yields the model

$$\begin{bmatrix}\dot{x}_o(t)\\ \dot{x}_{\bar{o}}(t)\end{bmatrix} = \begin{bmatrix}A_o & 0\\ A_{21} & A_{\bar{o}}\end{bmatrix}\begin{bmatrix}x_o(t)\\ x_{\bar{o}}(t)\end{bmatrix}$$
$$y(t) = \begin{bmatrix}C_o & 0\end{bmatrix}\begin{bmatrix}x_o(t)\\ x_{\bar{o}}(t)\end{bmatrix},$$

with $x_o(t) \in \mathbb{R}^{N_{x_o}}$ and $x_{\bar{o}}(t) \in \mathbb{R}^{(N_x - N_{x_o})}$. A sufficient and necessary condition for detectability is that $\mathtt{Re}(\lambda_j) < 0$ for all eigenvalues $\lambda_j \in \sigma(A_{\bar{o}}) \subset \sigma(A)$ (Callier and Desoer, 1991).

Though straightforward, these criteria are unpractical for high-dimensional systems as the design of P_c and P_o requires the computation of $\mathcal{C}$ and $\mathcal{O}$, respectively. Scalable alternatives are the Popov-Belevitch-Hautus tests for stabilisability and detectability: Necessary and sufficient conditions are

Lemma 8. *(Hautus, 1970). Let $\sigma(A) = \{\lambda_i\}_{i=1}^{N_x}$ be the spectrum of A and $\tilde{\sigma}(A) = \{\lambda_i \in \sigma(A) \mid \mathtt{Re}(\lambda_i) \geq 0\}$ be the set of eigenvalues with positive real part. The statement 'the pair (A, B) is stabilizable' is equivalent to the statements:*

$$\mathtt{rank}(\begin{bmatrix}\lambda I - A & B\end{bmatrix}) = N_x, \quad \forall \lambda \in \mathbb{C};$$
$$\mathtt{rank}(\begin{bmatrix}\lambda_i I - A & B\end{bmatrix}) = N_x, \quad \forall \lambda_i \in \tilde{\sigma}(A) \subset \mathbb{C}_{\geq 0}.$$

Lemma 9. *(Hautus, 1970). Let $\sigma(A) = \{\lambda_i\}_{i=1}^{N_x}$ be the spectrum of A and $\tilde{\sigma}(A) = \{\lambda_i \in \sigma(A) \mid \mathtt{Re}(\lambda_i) \geq 0\}$ be the set of eigenvalues with positive real part. The statement 'the pair (A, C) is detectable' is equivalent to the following statements:*

$$\mathtt{rank}(\begin{bmatrix}\lambda I - A^\mathsf{T} & C^\mathsf{T}\end{bmatrix}^\mathsf{T}) = N_x, \quad \forall \lambda \in \mathbb{C};$$
$$\mathtt{rank}(\begin{bmatrix}\lambda_i I - A^\mathsf{T} & C^\mathsf{T}\end{bmatrix}^\mathsf{T}) = N_x, \quad \forall \lambda_i \in \tilde{\sigma}(A) \subset \mathbb{C}_{\geq 0}.$$

Based on Lemma 8, (A, B) is stabilizable if and only if, for each unstable eigenvalue λ_i of A ($\mathtt{Re}(\lambda_i) \geq 0$ and $\mathtt{rank}(\lambda_i I - A) < N_x$), the columns of B have at least one component in the direction $\nu_i \in \mathbb{R}^{N_x}$, the eigenvector of A associated to λ_i. Notice that every system (A, B) with a stable matrix A is stabilizable, since $\tilde{\sigma}(A) = \emptyset$. Based on Lemma 9, (A, C) is detectable if and only if, for each unstable eigenvalue λ_i of A ($\mathtt{Re}(\lambda_i) \geq 0$ and $\mathtt{rank}(\lambda_i I - A^\mathsf{T}) < N_x$), the rows of C have at least one component in the direction of the eigenvector of A corresponding to λ_i, $\nu_i \in \mathbb{R}^{N_x}$. Every system (A, C) with a stable matrix A is detectable, since $\tilde{\sigma}(A) = \emptyset$.

4. The activated sludge plant: Structural and classical dynamical properties

In this section, we analyse the full-state controllability and observability properties for the class of activated sludge plants represented by Eq. (5) defined in Section 2. The presentation begins with the structural controllability and observability analysis of system (A, B, C) describing the structure of the ASP. A classical analysis of stability, controllability, and observability, is then performed for a standard linearisation (A^{SS}, B^{SS}, C^{SS}) of the model. A minimal realisation of this linearisation is also used to discuss the approximated system.

4.1. Structural properties

For the activated sludge plant $\dot{x}(t) = f(x(t), u(t), w(t)|\theta_x)$ with measurements $y(t) = g(x(t)|\theta_y)$ the structural matri-

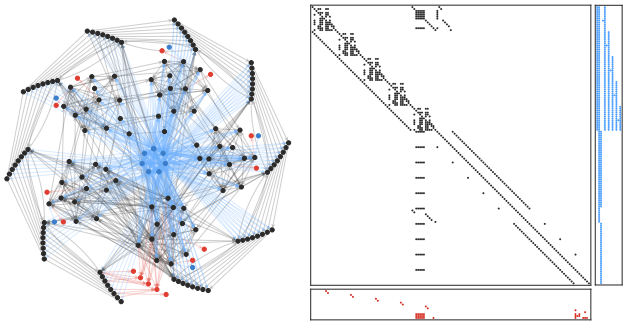

Figure 2: Network $\mathcal{G} = (\mathcal{V}, \mathcal{E})$ (left) for structured system (A, B, C) (right). State vertices $x_{n_x} \in \mathcal{V}_A$ are in black, input vertices $u_{n_u} \in \mathcal{V}_B$ in blue, and output vertices $y_{n_y} \in \mathcal{V}_C$ in red. State-state $(x_{n_x}, x_{n'_x}) \in \mathcal{E}_A$, input-state $(u_{n_u}, x_{n_x}) \in \mathcal{E}_B$, and state-output edges $(x_{n_x}, y_{n_y}) \in \mathcal{E}_C$ are dyed to match the corresponding entries in (A, B, C). Self-loops have been omitted.

ces $A \in \mathbb{R}^{N_x \times N_x}$, $B \in \mathbb{R}^{N_x \times N_u}$, and $C \in \mathbb{R}^{N_y \times N_x}$ are obtained from the Jacobians $A = \partial f/\partial x$, $B = \partial f/\partial u$, and $C = \partial g/\partial x$ with $N_x = 145$, $N_u = 13$ and $N_y = 15$. The associated digraph $\mathcal{G} = (\mathcal{V}, \mathcal{E})$ has the vertex and edge sets

$$\begin{aligned}\mathcal{V} &= \mathcal{V}_A \cup \mathcal{V}_B \cup \mathcal{V}_C \\ &= \{x_1, \dots, x_{N_x}\} \cup \{u_1, \dots, u_{N_u}\} \cup \{y_1, \dots, y_{N_y}\}; \quad (30a)\\ \mathcal{E} &= \mathcal{E}_A \cup \mathcal{E}_B \cup \mathcal{E}_C \\ &= \{(x_{n_x}, x_{n'_x}) \mid A_{n'_x, n_x} \neq 0\} \cup \{(u_{n_u}, x_{n_x}) \mid B_{n_x, n_u} \neq 0\} \\ &\quad \cup \{(x_{n_x}, y_{n_y}) \mid C_{n_y, n_x} \neq 0\}. \quad (30b)\end{aligned}$$

We discuss the structural controllability and observability of the pairs (A, B) and (A, C) and associated digraphs, Fig. 2.

4.1.1. Controllability and observability

The structural pair (A, B) associates with the directed subgraph $\mathcal{G}_c = (\mathcal{V}_c, \mathcal{E}_c)$, with $\mathcal{V}_c = \mathcal{V}_A \cup \mathcal{V}_B$ and $\mathcal{E}_c = \mathcal{E}_A \cup \mathcal{E}_B$. The topology of $\mathcal{G}_c = (\mathcal{V}_c, \mathcal{E}_c)$ shows that pair (A, B) is structurally controllable (Lemma 3). Accessibility is satisfied, all state vertices are reachable from a control vertex: All nodes are reachable through one-edge paths from control vertex Q_R or Q_W. Dilation-free is satisfied with a perfect matching $\mathcal{M}$ of size $|\mathcal{M}| = N_x$ formed by choosing every state vertex's self-loop, thus leaving no vertex unmatched. A perfect matching such as $\mathcal{M}$ ensures the dilation-free condition and suggests that controls are only needed to ensure accessibility.

The topology of $\mathcal{G}_c = (\mathcal{V}_c, \mathcal{E}_c)$ shows that (A, B) is not strongly structurally controllable: It is not possible to find a colouring for both graph $\mathcal{G}_c = (\mathcal{V}_c, \mathcal{E}_c)$ and modified graph $\widetilde{\mathcal{G}}_c = (\mathcal{V}_c, \widetilde{\mathcal{E}}_c)$ in which all vertices $x_{n_x} \in \mathcal{V}_A$ are coloured (Lemma 5). Being (A, B) not-controllable in a strong structural sense, there exist realisations of A and B for which the system is not controllable in a classical sense. Being structurally controllable, (A, B) is also controllable in a classical sense, for almost all possible realisations of A and B.

The structural pair (A, C) associates with the subgraph $\mathcal{G}_o = (\mathcal{V}_o, \mathcal{E}_o)$, with $\mathcal{V}_o = \mathcal{V}_A \cup \mathcal{V}_C$ and $\mathcal{E}_o = \mathcal{E}_A \cup \mathcal{E}_C$. The topology of $\mathcal{G}_o = (\mathcal{V}_o, \mathcal{E}_o)$ indicates that pair (A, C) is not structurally observable (Lemma 4). As there are no paths from state vertices $\{S_{ALK}^{A(r)}\}_{r=1}^{5}$, $\{S_{ALK}^{S(l)}\}_{l=1}^{10}$ and $\{S_O^{S(l)}\}_{l=7}^{10}$ to any of the output vertices, the accessibility condition is not satisfied. Conversely, the dilation-free condition is satisfied by the same perfect matching $\mathcal{M}$ of size $|\mathcal{M}| = N_x$ as before, obtained by choosing every state vertex's self-loop. The lack of structural observability implies non-observability in a classical sense.

The topology of $\mathcal{G}_o = (\mathcal{V}_o, \mathcal{E}_o)$ indicates that pair (A, C) is also not strongly structurally observable, an expected result.

4.1.2. Controllability and observability centrality

The relevance of each state node in the network can be quantified in terms of their in-degree and out-degree centrality.

Figure 3 shows how particulate $\{X_S^{A(r)}, X_{BA}^{A(r)}, X_{BH}^{A(r)}, X_P^{A(r)}, X_{ND}^{A(r)}\}_{r=1}^{1}$ and soluble components $\{S_{NH}^{A(r)}, S_{ALK}^{A(r)}\}_{r=1}^{5}$, are among the state vertices with highest in-degree centralities. This indicates that a large portion of the state-space is directly observed by a sensor measuring these state variables.

Similarly, particulate $\{X_S^{A(r)}, X_{BA}^{A(r)}, X_{BH}^{A(r)}, X_P^{A(r)}\}_{r=1}^{1}$ and oxygen $S_O^{A(1 \rightsquigarrow 5)}$, are also among the state vertices of highest out-degree centralities. Thus, a large portion of the network can be directly controlled by an input configuration that manipulates those variables. However, note that it is possible to control $S_O^{A(r)}$ (through $K_L a^{(r)}$), while individually controlling (or measuring) any of the concentrations $X_{BH}^{A(r)}$, $X_{BA}^{A(r)}$, $X_P^{A(r)}$, or $X_I^{A(r)}$, is practically unfeasible. Moreover, the species in the reactors have higher centralities than those in the settler.

We conclude that, for the activated sludge plant in Eq. (5), it is possible to design a control $u(\cdot)$ that transfers the plant to a desired state, in finite time, regardless of the realisation of (A, B). It is not possible, however, to determine an initial state $x(t_0)$, and thus neither intermediate states $x(t)$, from measurements $y(t_0 \rightsquigarrow t_f)$. As a result, it is not possible to design a full-state observer based on such measurements and model, whatever the realisation of (A, C). Being of structural nature, the conclusions are valid also in a classical sense.

4.2. Classical properties of a common linearisation

We now consider the linearisation (A^{SS}, B^{SS}, C^{SS}), corresponding to the fixed point $SS \equiv (x^{SS}, u^{SS}, w^{SS}, y^{SS})$ considered by Gernaey et al. (2014). This linearisation is commonly utilised in the literature and constitutes the default configuration of the BSM1. The matrices $A^{SS} \in \mathbb{R}^{N_x \times N_x}$, $B^{SS} \in \mathbb{R}^{N_x \times N_u}$, and $C^{SS} \in \mathbb{R}^{N_y \times N_x}$ are obtained from the Jacobians evaluated at such equilibrium point $A^{SS} = (\partial f/\partial x)|_{SS}$, $B^{SS} = (\partial f/\partial u)|_{SS}$, and $C^{SS} = (\partial g/\partial x)|_{SS}$.

The, now weighted, associated digraph $\mathcal{G}_{SS} = (\mathcal{V}_{SS}, \mathcal{E}_{SS})$,

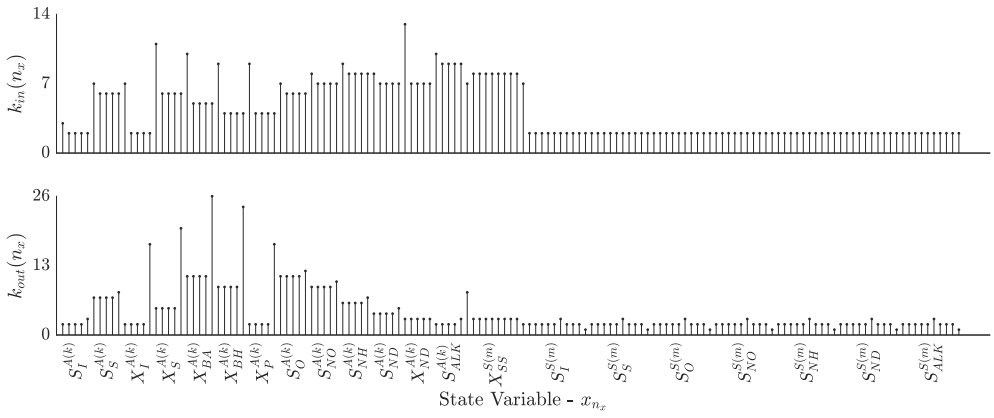

Figure 3: Network $\mathcal{G} = (\mathcal{V}, \mathcal{E})$: In-degree, $k_{in}(n_x)$, and out-degree, $k_{out}(n_x)$, centralities associated to each state node $x_{n_x} \in \mathcal{V}_A$.

shown at Fig. 4, is defined by the vertex and edge sets

$$\begin{aligned}\mathcal{V}_{SS} &= \mathcal{V}_{A^{SS}} \cup \mathcal{V}_{B^{SS}} \cup \mathcal{V}_{C^{SS}} \\ &= \{x_1, \dots, x_{N_x}\} \cup \{u_1, \dots, u_{N_u}\} \cup \{y_1, \dots, y_{N_y}\} \\ \mathcal{E}_{SS} &= \mathcal{E}_{A^{SS}} \cup \mathcal{E}_{B^{SS}} \cup \mathcal{E}_{C^{SS}} \\ &= \{(x_{n_x}, x_{n'_x}) \mid A^{SS}_{n'_x, n_x} \neq 0\} \cup \{(u_{n_u}, x_{n_x}) \mid B^{SS}_{n_x, n_u} \neq 0\} \\ &\quad \cup \{(x_{n_x}, y_{n_y}) \mid C^{SS}_{n_y, n_x} \neq 0\}.\end{aligned}$$

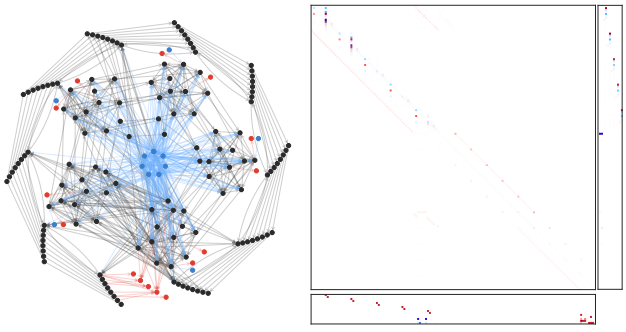

Figure 4: Network $\mathcal{G}_{SS} = (\mathcal{V}_{SS}, \mathcal{E}_{SS})$ (left) associated to linearisation (A^{SS}, B^{SS}, C^{SS}) (right). State vertices $x_{n_x} \in \mathcal{V}_{A^{SS}}$ and state-state edges $(x_{n_x}, x_{n'_x}) \in \mathcal{E}_{A^{SS}}$ are in black, input vertices $u_{n_u} \in \mathcal{V}_{B^{SS}}$ and input-state edges $(u_{n_u}, x_{n_x}) \in \mathcal{E}_{B^{SS}}$ are in blue, and output vertices $y_{n_y} \in \mathcal{V}_{C^{SS}}$ and state-output edges $(x_{n_x}, y_{n_y}) \in \mathcal{E}_{C^{SS}}$ are in red. State self-loops have been omitted.

We discuss the stability of (A^{SS}, B^{SS}, C^{SS}) and the classic controllability and observability properties of (A^{SS}, B^{SS}) and (A^{SS}, C^{SS}). For completeness, we use the approximation to validate the structural results that we reported earlier.

4.2.1. Stability

The spectrum of A^{SS} consists of 69 distinct eigenvalues and associated eigenvectors, $\sigma(A^{SS}) = \{\lambda_i(A^{SS}), \nu_i(\lambda_i)\}_{i=1}^{69}$, with $\{\lambda_1, \cdots, \lambda_{31}\} \subset \mathbb{R}$ and $\{(\lambda_{32}, \lambda^*_{32}), \cdots, (\lambda_{69}, \lambda^*_{69})\} \subset \mathbb{C}$, Fig. 5. Five complex conjugate pairs of eigenvalues have algebraic multiplicity equal to two and two distinct real eigenvalues have algebraic multiplicities equal to two and twenty-eight, respectively. The distribution of eigenvalues in the complex plane shows that most of the modes have relatively slow time constants. As most eigenvalues are close to the real axis, pseudo-oscillatory behaviour is barely noticeable.

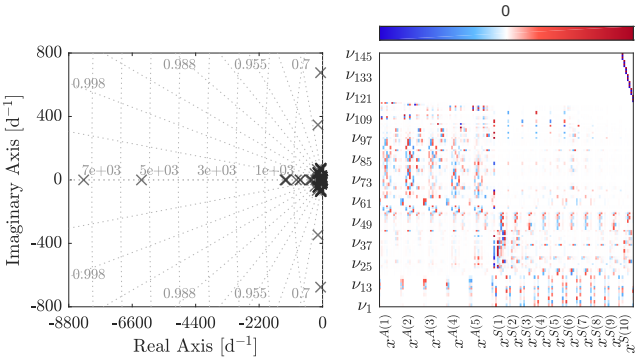

Figure 5: Spectrum $\sigma(A^{SS})$: Eigenvalues $\lambda_i \in \sigma(A^{SS})$ and associated eigenvectors $\nu_i(\lambda_i)$ (left and right panels, respectively). The grid in the complex plane displays lines corresponding to constant damping factors (diagonal lines) and natural frequencies (vertical lines, in rad/days) for the associated modes.

Being $\mathrm{Re}(\lambda_i) < 0$ for all $\lambda_i \in \sigma(A^{SS})$, then A^{SS} is Hurwitz and (A^{SS}, B^{SS}, C^{SS}) is asymptotically stable (Section 3.1). This result can also be visualised through the simulation of individual system modes, shown in Fig. 6. As the unforced evolution of the system, from any $x(0)$, is a linear combination of system modes, the fact that all curves converge to zero further confirms that the system is asymptotically stable.

4.2.2. Controllability and observability

Regarding the controllability of pair (A^{SS}, B^{SS}) and associated digraph $\mathcal{G}_{cSS} = (\mathcal{V}_{cSS}, \mathcal{E}_{cSS})$, with $\mathcal{V}_{cSS} = \mathcal{V}_{A^{SS}} \cup \mathcal{V}_{B^{SS}}$ and $\mathcal{E}_{cSS} = \mathcal{E}_{A^{SS}} \cup \mathcal{E}_{B^{SS}}$, the topology of the network indicates that (A^{SS}, B^{SS}, C^{SS}) is controllable in a structural sense (Lemma 3). Because pair (A^{SS}, B^{SS}) corresponds to the linear time-invariant approximation of Eq. (5a) about steady-state point SS, it is possible to study its controllability also in a conventional sense. Classical

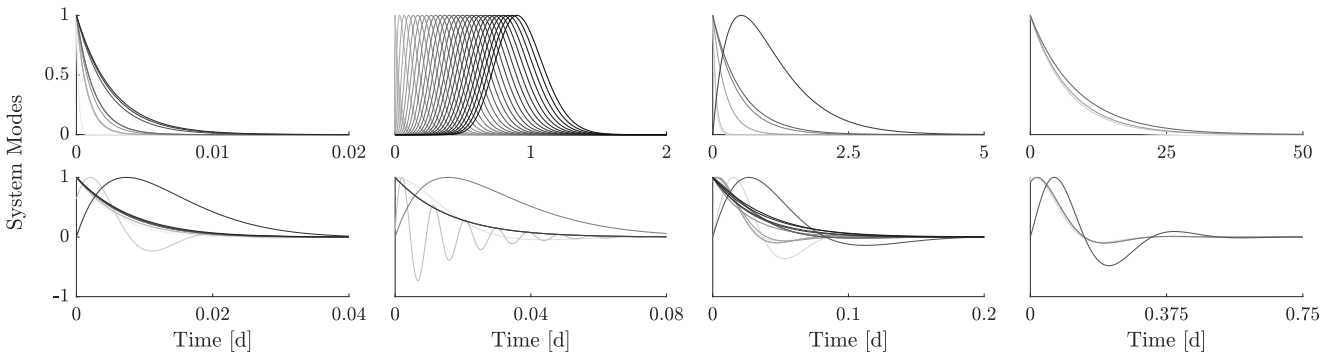

Figure 6: The normalised modes $t^k e^{\lambda_i t}/\max_t t^k e^{\lambda_i t}$ $(k = 0, \cdots, \mu(\lambda_i) - 1)$ for the real eigenvalues (top) and complex conjugated pairs of eigenvalues (bottom) from the spectrum $\sigma(A^{SS}) = \{\lambda_i, \nu_i(\lambda_i)\}_{i=1}^{N_x}$. Grouping is based on each mode's time constant $\tau_i = 1/\mathtt{Re}[\lambda_i]$.

controllability can be verified with a PBH test (Lemma 1), as an accurate computation of the controllability matrix $\mathcal{C} = [B^{SS}\ A^{SS}B^{SS}\ \cdots\ (A^{SS})^{N_x-1}B^{SS}]$ is ill-posed.

Surprisingly, the PBH test contradicts the structural result and returns that (A^{SS}, B^{SS}) is not controllable in the classical sense. Specifically, a real eigenvalue with algebraic multiplicity equal to 28 leads to a rank-deficient matrix $[\lambda_i I - A^{SS}\ B^{SS}]$. The twenty-eight associated eigenvectors are shown in Fig. 7, top. Interestingly, the non-zero entries of the eigenvectors correspond to state variables relative to soluble matter in the settler's last layer, showing that it is not possible to synthesise a control $u(\cdot)$ that enforces a desired profile of soluble matter in the settler. As A^{SS} is Hurwitz the eigenvalue failing the PBH test satisfies $\mathtt{Re}(\lambda_i) < 0$ indicating that the pair (A^{SS}, B^{SS}) is stabilizable (Lemma 8). The apparent contradiction between classical and structural controllability results is explained in Subsection 4.3.

Observability of the pair (A^{SS}, C^{SS}) and associated digraph $\mathcal{G}_{oSS} = (\mathcal{V}_{oSS}, \mathcal{E}_{oSS})$, with $\mathcal{V}_{oSS} = \mathcal{V}_{ASS} \cup \mathcal{V}_{CSS}$ and $\mathcal{E}_{oSS} = \mathcal{E}_{ASS} \cup \mathcal{E}_{CSS}$ indicates that also the pair (A^{SS}, B^{SS}, C^{SS}) is not observable in a structural sense, as there is still no directed path from the state vertices $\{S_{ALK}^{A(r)}\}_{r=1}^{5}$, $\{S_{ALK}^{S(l)}\}_{l=1}^{10}$ and $\{S_O^{S(l)}\}_{l=7}^{10}$ to any of the output vertices. Similarly, classical observability of (A^{SS}, C^{SS}) can be verified only with the PBH test (Lemma 2), because of the limitations in the computation of $\mathcal{O} = [C^{SS^\mathsf{T}}\ A^{SS^\mathsf{T}}C^{SS^\mathsf{T}}\ \cdots\ (A^{SS^\mathsf{T}})^{N_x-1}C^{SS^\mathsf{T}}]^\mathsf{T}$.

The PBH test confirms that the pair (A^{SS}, C^{SS}) is not observable. Ten distinct eigenvalues, including two real ones with multiplicities equal to two and twenty-eight, respectively, and five complex conjugated pairs with multiplicities equal to two lead to rank-deficient matrices $[\lambda_i I - A^{SS^\mathsf{T}}\ C^{SS^\mathsf{T}}]^\mathsf{T}$. The forty-three associated eigenvectors are shown in Fig. 7, bottom. As before, the non-zero entries of the eigenvectors associated to one of the real eigenvalues refer to state variables relative to effluent soluble matter. From the remaining fifteen eigenvectors, three have non-zero entries only at state variables $\{X_I^{A(r)}, X_P^{A(r)}\}_{r=1}^{5}$, while the other twelve have non-zero entries only at state variables $\{S_I^{A(r)}, S_{ALK}^{A(r)}\}_{r=1}^{5}$ and $\{S_I^{S(l)}, S_{ALK}^{S(l)}\}_{l=1}^{10}$. Interestingly, these correspond to concentrations of non-reacting matter. Because A^{SS} is a stable matrix, all eigenvalues failing the PBH test satisfy $\mathtt{Re}(\lambda_i) < 0$, thus rendering the pair (A^{SS}, C^{SS}) detectable (Lemma 9).

We conclude that for the approximation (A^{SS}, B^{SS}, C^{SS}) it is not possible to design a control $u(\cdot)$ that transfers the plant to any state $x(t_f)$ in finite time. Moreover, it is also not possible to determine the initial state $x(t_0)$, and thus neither intermediate states $x(t)$, from measurements $y(t_0 \rightsquigarrow t_f)$.

4.2.3. Controllability and observability metrics and minimal realisation

To provide a qualitative analysis of controllability and observability, we firstly analyse the effort associated with controlling or observing each state variable individually. Then, we analysise a minimal realisation of lienarisation (A^{SS}, B^{SS}, C^{SS}).

Considering the linearisation (A^{SS}, B^{SS}, C^{SS}), the average energy that is required to respectively control or reconstruct the full-state by directly controlling or measuring only one individual state variable is quantified by its average controllability and average observability centralities, in Fig. 8.

Our results show that the energy required to reach any point in the entire state-space is among the lowest if we were to actuate on control variables only affecting biomass ($X_{BH}^{A(r)}$, $X_{BA}^{A(r)}$, and $X_P^{A(r)}$) or particulate inert organic matter ($X_I^{A(r)}$) in the reactors. This reflects the fact that such variables are central to the process, but will evolve slowly if not controlled. Conversely, the required energy would be the highest if we were to actuate on controls only affecting dissolved oxygen ($S_O^{A(r)}$). Again, it is worth mentioning that it is still possible to control $S_O^{A(r)}$ (through $K_L a^{(r)}$), whereas individually controlling any of the concentrations $X_{BH}^{A(r)}$, $X_{BA}^{A(r)}$, $X_P^{A(r)}$, or $X_I^{A(r)}$, is practically unfeasible. The analysis also shows that acting directly on most state variables in the reactors is less demanding than acting on any state variables in the settler.

Our results also show that the effort required to reconstruct any point in the entire state-space is the lowest if we were to directly measure suspended solids at the bottom of the settler

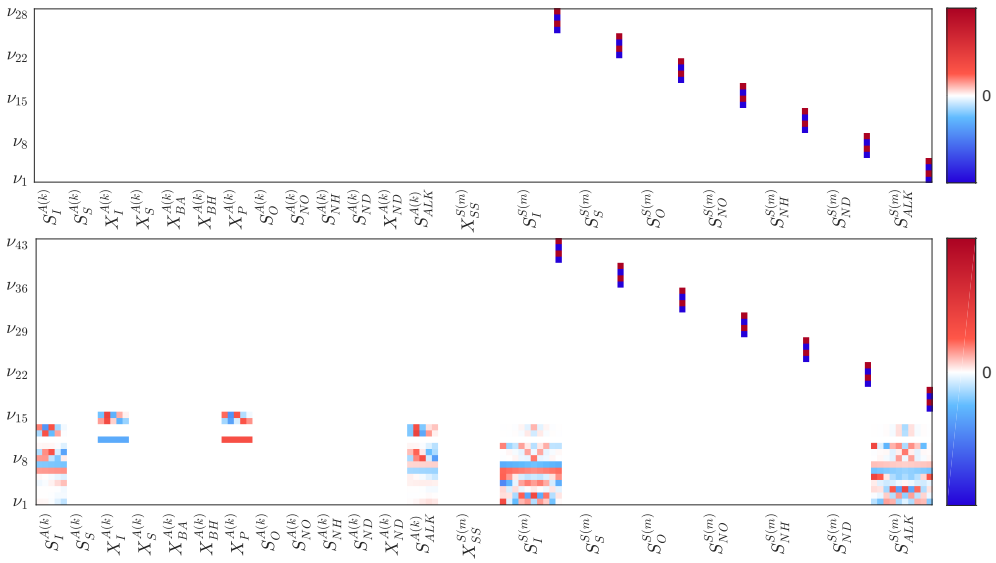

Figure 7: System (A^{SS}, B^{SS}, C^{SS}): Eigenvectors $\nu_i(\lambda_i)$ associated with eigenvalues $\lambda_i \in \sigma(A^{SS})$ failing the PBH controllability test ($\mathrm{rank}([\lambda_i I - A^{SS} \; B^{SS}]) < N_x$), top; and $\lambda_i \in \sigma(A^{SS})$ failing the PBH observability test ($\mathrm{rank}([\lambda_i I - A^{SS^\mathsf{T}} \; C^{SS^\mathsf{T}}]^\mathsf{T}) < N_x$), bottom.

$(X_{SS}^{S(1)})$. Additionally, the effort required is also among the lowest if we were to directly measure biomass ($X_{BH}^{A(r)}$, $X_{BA}^{A(r)}$, and $X_P^{A(r)}$) and particulate inert organic matter ($X_I^{A(r)}$) in the reactors. Again, this confirms the importance of measuring such variables and how reconstructing the state is more demanding when they are not available. In practice, only dissolved oxygen ($S_O^{A(r)}$) and nitrate and nitrite nitrogen ($S_{NO}^{A(r)}$) in each reactor, along with NH_4^++NH_3 nitrogen in the effluent ($S_{NH}^{S(10)}$), are directly measured. These variables are associated with the highest measurement effort if used individually to reconstruct the entire state of the process.

To complete the analysis of (A^{SS}, B^{SS}, C^{SS}), we study the compound energy-related metrics for the control and measurement configuration. Being the linearisation both uncontrollable and unobservable, these Gramian-based metrics of (A^{SS}, B^{SS}, C^{SS}) will obviously conclude that its control or state reconstruction are infinitely demanding. Alternatively, we further analyse (A^{SS}, B^{SS}, C^{SS}) using a minimal realisation (Lemma 7), as it preserves its input-output behaviour,

$$\begin{aligned} \dot{x}_{co}(t) &= A_{co}x_{co}(t) + B_{co}u(t) \\ y(t) &= C_{co}x_{co}(t), \end{aligned}$$

with $A_{co} \in \mathbb{R}^{N_{x_{co}} \times N_{x_{co}}}$, $B_{co} \in \mathbb{R}^{N_{x_{co}} \times N_u}$ and $C_{co} \in \mathbb{R}^{N_y \times N_{x_{co}}}$, for $N_{x_{co}} = 117$. Note that, because $\sigma(A_{co}) \subseteq \sigma(A^{SS})$, it follows that $\mathrm{Re}(\lambda_i) < 0$ for all eigenvalues $\lambda_i \in \sigma(A_{co})$, and the minimal realisation (A_{co}, B_{co}, C_{co}) is stable.

We analysed the energy-related metrics defined for the infinite-horizon controllability ($W_c(\infty)$) and observability ($W_o(\infty)$) Gramians (Section 3.2.1). As the state matrix is Hurwitz, these Gramians are computed by solving Lyapunov equations $A_{co}W_c(\infty) + W_c(\infty)A_{co}^\mathsf{T} = -B_{co}B_{co}^\mathsf{T}$ and $W_o(\infty)A_{co}^\mathsf{T} + A_{co}W_o(\infty) = -C_{co}^\mathsf{T}C_{co}$. The metrics (Table 2) reveal that controlling and observing this system is difficult, even for a minimal realisation. Specifically, the fact that $\lambda_{min}(W_c(\infty))$ and $\lambda_{min}(W_o(\infty))$ are virtually zero implies the existence of state-space directions which are unaccessible.

Table 2
System (A_{co}, B_{co}, C_{co}): Energy-related metrics.

	$\mathrm{trace}(W)$	$\mathrm{trace}(W^\dagger)$	$\log(\det(W))$	$\lambda_{\min}(W)$
$W_c(\infty)$	$1.23 \cdot 10^5$	$1.36 \cdot 10^9$	$-\infty$	$1.01 \cdot 10^{-11}$
$W_o(\infty)$	0.52	$6.76 \cdot 10^{14}$	$-\infty$	$5.69 \cdot 10^{-19}$

We conclude that, though formally controllable and observable, the realisation (A_{co}, B_{co}, C_{co}) requires large control and measurement efforts. The cumulative coverage of the minimal state-space is shown in terms of a normalised cumulative sum ($\Lambda(N) = \sum_{n=1}^{N} \lambda_n / \sum_{n_x=1}^{N_{x_{co}}} \lambda_{n_x}$) for the (sorted) eigenvalues of $W_c(\infty)$ and $W_o(\infty)$, Fig. 8. As more than 90% of the coverage is reached with a small number of eigenvalules, the state-space coverage implies that most of the control and output energy are comprised within a small number of directions. Together with Table 2, this shows that the input-output behaviour is mostly described by a small number of state-space directions, some of which being virtually inaccessible.

4.3. About the contradiction between structural and classical controllability results

When studying the controllability of (A^{SS}, B^{SS}, C^{SS}), we have shown that (A^{SS}, B^{SS}) is controllable in a structural but not in a classical sense, a result that could be anticipated by the fact that (A, B) is not controllable in a strong structural sense. We further explain the apparent contradiction from the analysis of the dilation-free condition on $\mathcal{G}_{c^{SS}} = (\mathcal{V}_{c^{SS}}, \mathcal{E}_{c^{SS}})$.

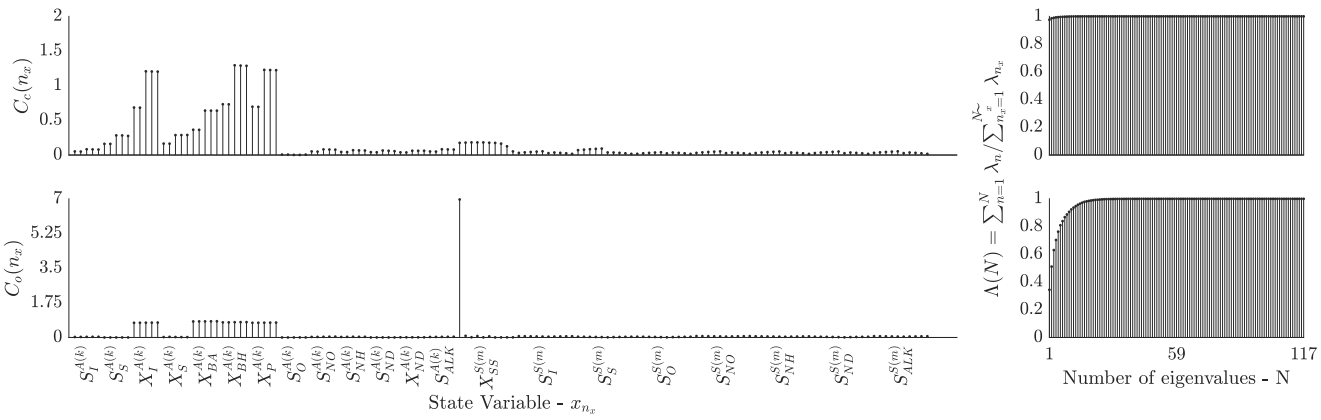

Figure 8: System (A^{SS}, B^{SS}, C^{SS}): On the left, the average controllability centrality $C_c(n_x)$, top, and average observability centrality $C_o(n_x)$, bottom, associated to each state variable x_{n_x} $(n_x = 1, \dots, N_x)$. On the right, the cumulative sum $\Lambda(N)$ for the eigenvalues of the infinite-horizon controllability Gramian $W_c(\infty)$, top, and the infinite-horizon observability Gramian $W_o(\infty)$, bottom.

Specifically, as the existence of a self-loop for each state vertex is sufficient to satisfy the dilation-free condition, input vertices are needed only to satisfy the accessibility condition. Whenever some of the self-loop weights are equal, the dilation-free condition will underestimate the controls needed for full-state controllability (Zhao et al., 2015). This is the case for (A^{SS}, B^{SS}), where all reactors' non-reacting components (respectively, all settler's soluble components) from the same unit (layer) always have identical self-dynamics.

Consider non-reacting components $S_a^{A(r)}$ $(a \in \{I, ALK\})$ and $X_b^{A(r)}$ $(b \in \{I, P\})$ in the r-th reactor. For all $r = 1, \dots, 5$, their dynamics in Eq. (5a) are each of the form $\dot{S}_a^{A(r)} = Q^{A(r)}(S_a^{A(r-1)} - S_a^{A(r)}) - (Q_{EC}^{(r)}/V^{(r)})S_a^{A(r)} + R_a^{(r)}$ and $\dot{X}_b^{A(r)} = Q^{A(r)}(X_b^{A(r-1)} - X_b^{A(r)}) - (Q_{EC}^{(r)}/V^{(r)})X_b^{A(r)} + R_b^{(r)}$, with $Q^{A(r)}$ denoting influent flow-rates and $R_a^{(r)}$ and $R_b^{(r)}$ indicating the contribution from reactions. The model assumes equal influent flow-rates, $\{Q^{A(r)} = (Q_A + Q_R + Q_{IN} + \sum_{j=1}^{r-1} Q_{EC}^{(j)})/V_A^{(r)}\}_{r=1}^{5}$, and constant volumes $V_A^{(1\rightsquigarrow 2)} = 1000\ \mathrm{m}^3$ and $V_A^{(3\rightsquigarrow 5)} = 1333\ \mathrm{m}^3$. As $S_a^{A(r)}$ and $X_b^{A(r)}$ are non-reacting, we have $\partial R_a^{(r)}/\partial S_a^{A(r)} = \partial R_b^{(r)}/\partial X_b^{A(r)} = 0$. For the relevant entries in the Jacobian $\partial f/\partial x$, we have

$$\left.\frac{\partial \dot{S}_a^{A(r)}}{\partial S_a^{A(r)}}\right|_{SS} = \left.\frac{\partial \dot{X}_b^{A(r)}}{\partial X_b^{A(r)}}\right|_{SS} = -\left.\frac{Q_A + Q_R + Q_{IN} + \sum_{j=1}^{r} Q_{EC}^{(j)}}{V_A^{(r)}}\right|_{SS},$$

which is equal for all reactors, regardless of fixed-point SS.

Similarly, the dynamics of the soluble components $S_c^{S(l)}$ $(c \in \{I, S, O, NO, NH, ND, ALK\})$ in the l-th layer of the settler are each represented in Eq. (5a) by first-order differential equations of the form $\dot{S}_c^{S(l)} = Q^{S(l)}(S_c^{S(l')} - S_c^{S(l)})$, for $l = 1, \dots, 10$. $Q^{S(l)}$ denotes the influent flow-rate to the l-th layer. The model assumes a same influent flow-rate for all upper layers, $\{Q^{S(l)} = (Q_{IN} - Q_W)/V_S^{(l)}\}_{l=7}^{10}$, for all lower layers, $\{Q^{S(l)} = (Q_R + Q_W)/V_S^{(l)}\}_{l=1}^{5}$, and for the feed layer we have $Q^{S(6)} = (Q_{IN} + Q_R)/V_S^{(l)}$. The model also assumes constant volume hold-ups $V_S^{(l)} = 600\ \mathrm{m}^3$.

For the relevant entries in the Jacobian matrix $\partial f/\partial x$,

$$\left.\frac{\partial \dot{S}_c^{S(l)}}{\partial S_c^{S(l)}}\right|_{SS} = \begin{cases} -(Q_{IN} - Q_W)/V_S^{(l)}\big|_{SS} & (l = 7, \cdots, 10) \\ -(Q_{IN} + Q_R)/V_S^{(l)}\big|_{SS} & (l = 6) \\ -(Q_R + Q_W)/V_S^{(l)}\big|_{SS} & (l = 1, \cdots, 5) \end{cases},$$

which is equal for all components, whatever the fixed-point.

5. The activated sludge plant: Properties of certain alternative control configurations

We complete our study with an analysis of two alternative configurations of the activated sludge plant defined in Section 2. We firstly study the ASP when the Takács' model of the settler is replaced by a simpler 3-layer model with the same structure, while retaining our setup for the sensors and actuators. Secondly, we consider the ASP with the full process model under the minimal configuration of sensors and actuators as proposed in the original benchmark.

5.1. The ASP with a simplified model for the settler

Because of the impossibility to reach any desired concentration profile along the settler with the given controls (Section 4.2.2), we are interested in a potentially controllable representation with a reduced number of identical self-dynamics.

We consider a 3-layer model of the settler for the concentrations of soluble matter: The layers are top, feed, and bottom ones. The variables related to soluble matter in the l-th layer are $\tilde{x}^{S(l)} = (S_I^{S(l)}, S_S^{S(l)}, S_O^{S(l)}, S_{NO}^{S(l)}, S_{NH}^{S(l)}, S_{ND}^{S(l)}, S_{ALK}^{S(l)})$,

$$\dot{\tilde{x}}(t) = \tilde{f}(\tilde{x}(t), u(t), w(t)|\theta_x); \tag{32a}$$

$$y(t) = g(\tilde{x}(t)|\theta_y), \tag{32b}$$

consists of $N_{\tilde{x}} = 13{\times}5{+}10{+}7{\times}3 = 96$ state variables $\tilde{x}(t) = \left((x^{A(1)}, \cdots, x^{A(5)}), (X_{SS}^{S(1)}, \cdots, X_{SS}^{S(10)}, \tilde{x}^{S(1)}, \tilde{x}^{S(6)}, \tilde{x}^{S(10)})\right)^{\mathsf{T}} \in \mathbb{R}_{\geq 0}^{N_{\tilde{x}}}$. Inputs $u(t) \in \mathbb{R}_{\geq 0}^{N_u}$ and $w(t) \in \mathbb{R}_{\geq 0}^{N_w}$, and the outputs $y(t) \in \mathbb{R}_{\geq 0}^{N_y}$ are unchanged: $N_u = 13$, $N_w = 14$, $N_y = 15$.

The structural realisation of matrices $A_s \in \mathbb{R}^{N_{\tilde{x}} \times N_{\tilde{x}}}$, $B_s \in \mathbb{R}^{N_{\tilde{x}} \times N_u}$, and $C_s \in \mathbb{R}^{N_y \times N_{\tilde{x}}}$ can be obtained as $A_s = \partial \tilde{f}/\partial \tilde{x}$, $B_s = \partial \tilde{f}/\partial u$, and $C_s = \partial g/\partial \tilde{x}$. The digraph $\mathcal{G}_s = (\mathcal{V}_s, \mathcal{E}_s)$ associated to (A_s, B_s, C_s), Fig. 9, has vertex and edge sets

$$\begin{aligned}
\mathcal{V}_s &= \mathcal{V}_{A_s} \cup \mathcal{V}_{B_s} \cup \mathcal{V}_{C_s} \\
&= \{x_1, \ldots, x_{N_{\tilde{x}}}\} \cup \{u_1, \ldots, u_{N_u}\} \cup \{y_1, \ldots, y_{N_y}\}; \\
\mathcal{E}_s &= \mathcal{E}_{A_s} \cup \mathcal{E}_{B_s} \cup \mathcal{E}_{C_s} \\
&= \{(x_{n_x}, x_{n'_x}) \mid [A_s]_{n'_x, n_x} \neq 0\} \cup \{(u_{n_u}, x_{n_x}) \mid [B_s]_{n_x, n_u} \neq 0\} \\
&\quad \cup \{(x_{n_x}, y_{n_y}) \mid [C_s]_{n_y, n_x} \neq 0\}.
\end{aligned}$$

The numerical realisation $(A_s^{SS}, B_s^{SS}, C_s^{SS})$ is obtained for the usual equilibrium point $SS \equiv (x^{SS}, u^{SS}, w^{SS}, y^{SS})$ of Gernaey et al. (2014) by evaluating the Jacobians: $A_s^{SS} = \partial \tilde{f}/\partial \tilde{x}|_{SS}$, $B_s^{SS} = \partial \tilde{f}/\partial u|_{SS}$, and $C_s^{SS} = \partial g/\partial \tilde{x}|_{SS}$.

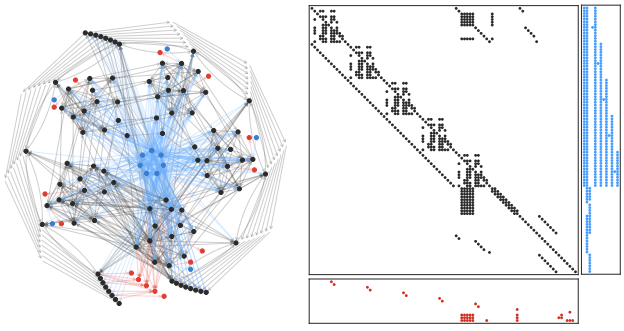

Figure 9: Network $\mathcal{G}_s = (\mathcal{V}_s, \mathcal{E}_s)$ (left) associated to (A_s, B_s, C_s) (right). State vertices $x_{n_x} \in \mathcal{V}_{A_s}$ are in black, input vertices $u_{n_u} \in \mathcal{V}_{B_s}$ are in blue, and output vertices $y_{n_y} \in \mathcal{V}_{C_s}$ are in red. State-state edges $(x_{n_x}, x_{n'_x}) \in \mathcal{E}_{A_s}$, input-state edges $(u_{n_u}, x_{n_x}) \in \mathcal{E}_{B_s}$, and state-output edges $(x_{n_u}, y_{n_y}) \in \mathcal{E}_{C_s}$ are dyed to match the corresponding entries in (A_s, B_s, C_s). Self-loops are omitted.

We discuss the properties of the realisations (A_s, B_s, C_s) and $(A_s^{SS}, B_s^{SS}, C_s^{SS})$ associated to this simplified model. We show that the system is now controllable, but it is still unobservable, in both a structural and in a classical sense.

5.1.1. Structural Analysis

Controllability: The structural pair (A_s, B_s) associates with subgraph $\mathcal{G}_{s^c} = (\mathcal{V}_{s^c}, \mathcal{E}_{s^c})$, with $\mathcal{V}_{s^c} = \mathcal{V}_{A_s} \cup \mathcal{V}_{B_s}$ and $\mathcal{E}_{s^c} = \mathcal{E}_{A_s} \cup \mathcal{E}_{B_s}$. The topology of $\mathcal{G}_{s^c} = (\mathcal{V}_{s^c}, \mathcal{E}_{s^c})$ indicates that pair (A_s, B_s) is structurally controllable (Lemma 3). The accessibility condition is satisfied since all state vertices are reachable from a control vertex: Specifically, it is possible to see how the state nodes all are reachable through directed paths from either control vertex Q_R or Q_W. The dilation-free condition is satisfied through a perfect matching $\mathcal{M}$ of size $|\mathcal{M}| = N_{\tilde{x}}$ formed by choosing every state vertex's self-loop.

The topology of $\mathcal{G}_{s^c} = (\mathcal{V}_{s^c}, \mathcal{E}_{s^c})$ also shows that pair (A_s, B_s) is not strongly structurally controllable (Section 3.2.2): It is not possible to find a colouring for both graph $\mathcal{G}_{s^c} = (\mathcal{V}_{s^c}, \mathcal{E}_{s^c})$ and modified graph $\widetilde{\mathcal{G}}_{s^c} = (\mathcal{V}_{s^c}, \widetilde{\mathcal{E}}_{s^c})$ in which all state nodes $x_{n_x} \in \mathcal{V}_A$ are coloured (Lemma 5). Being not strongly structurally controllable, there exist certain realisations of A_s and B_s for which the system is uncontrollable in a classical sense.

Observability: The structural pair (A_s, C_s) associates with subgraph $\mathcal{G}_{s^o} = (\mathcal{V}_{s^o}, \mathcal{E}_{s^o})$, with $\mathcal{V}_{s^o} = \mathcal{V}_{A_s} \cup \mathcal{V}_{C_s}$ and $\mathcal{E}_{s^o} = \mathcal{E}_{A_s} \cup \mathcal{E}_{C_s}$. The topology of $\mathcal{G}_{s^o} = (\mathcal{V}_{s^o}, \mathcal{E}_{s^o})$ indicates that pair (A_s, C_s) is structurally unobservable (Lemma 4). As there are still no paths from state vertices $\{S_{ALK}^{A(r)}\}_{r=1}^{5}$, $\{S_{ALK}^{S(l)}\}_{l=[1,6,10]}$ and $S_O^{S(10)}$ to any of the output vertices, the accessibility condition is not satisfied. The dilation-free condition is still satisfied through a perfect matching $\mathcal{M}$ of choosing every state vertex's self-loop. The topology of $\mathcal{G}_{s^o} = (\mathcal{V}_{s^o}, \mathcal{E}_{s^o})$ also indicates that the structural pair (A_s, C_s) is not strongly structurally observable, an expected result.

5.1.2. Classical analysis

Controllability: The controllability of pair (A_s^{SS}, B_s^{SS}) can be verified using the PBH controllability test (Lemma 1), as an accurate computation of the controllability matrix $\mathcal{C}_s = [B_s^{SS}\ A_s^{SS}B_s^{SS}\ \cdots\ (A_s^{SS})^{N_{\tilde{x}}-1}B_s^{SS}]$ is unfeasible also for this system. As $[\lambda_i I - A_s^{SS}\ B_s^{SS}]$ is full-rank for all eigenvalues $\lambda_i \in \sigma(A_s^{SS})$, pair (A_s^{SS}, B_s^{SS}) is controllable.

Observability: The observability of (A_s^{SS}, C_s^{SS}) can be verified using the PBH observability test (Lemma 2), again because an accurate computation of the observability matrix $\mathcal{O}_s = [C_s^{\mathsf{T}}\ A_s^{SS^{\mathsf{T}}}C_s^{SS^{\mathsf{T}}}\ \cdots\ (A_s^{SS^{\mathsf{T}}})^{N_{\tilde{x}}-1}C_s^{SS^{\mathsf{T}}}]^{\mathsf{T}}$ is unfeasible. The test confirms that (A_s^{SS}, C_s^{SS}) is not full-state observable, as ten distinct eigenvalues, including two real values with multiplicities equal to two, a real value with multiplicity seven, and two complex conjugated pairs with multiplicities equal to two, lead to rank-deficient matrices $[\lambda_i I - A_s^{SS^{\mathsf{T}}}\ C_s^{SS^{\mathsf{T}}}]^{\mathsf{T}}$.

The twenty eigenvectors associated to such eigenvalues are depicted in Fig. 10. The nonzero entries of these eigenvectors relate to the same state variables associated to nonzero entries of the eigenvectors from the PBH test of (A^{SS}, C^{SS}), Fig. 7.

5.1.3. Results

We conclude that for the activated sludge plant with a simplified model for the settler, it is possible to design a control $u(\cdot)$ that transfers the system to any desired state, in finite time. This is true for almost any possible realisation of (A_s, B_s). It is not possible, however, to determine the initial state $\tilde{x}(t_0)$, and thus neither intermediate states $\tilde{x}(t)$, starting from a se-

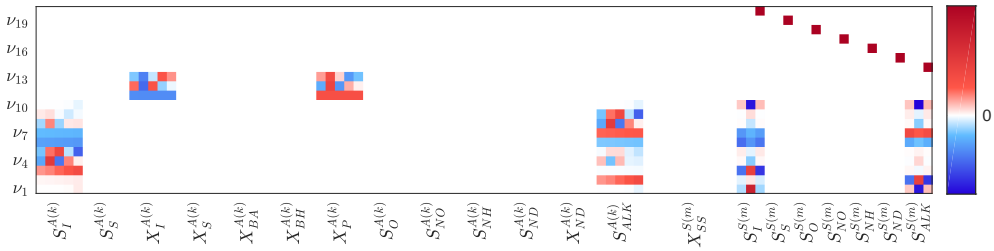

Figure 10: Pair (A_s^{SS}, C_s^{SS}): Eigenvectors $v_i(\lambda_i)$ with $\lambda_i \in \sigma(A_s^{SS})$ failing the PBH observability test $(\mathrm{rank}([\lambda_i I - A_s^{SS^\mathsf{T}} \; C_s^{SS^\mathsf{T}}]^\mathsf{T}) < N_{\tilde{x}})$.

quence of measurements $y(t_0 \rightsquigarrow t_f)$. Thus, it is also not possible to design a full-state-observer based on the existing measurements, no matter what realisation of (A_s, C_s) is used.

Being of structural nature, these conclusions are valid also in a classical sense, regardless of the linearisation. For the linearisation $(A_s^{SS}, B_s^{SS}, C_s^{SS})$, it is possible to design a control $u(\cdot)$ that is capable to transfers the system to a desired state $\tilde{x}(t_f)$ in finite time. It is not possible, however, to determine $\tilde{x}(t_0)$ and the intermediate states $\tilde{x}(t)$, from $y(t_0 \rightsquigarrow t_f)$.

5.2. BSM1's actuator and sensor configuration

We further consider the ASP with the minimal set of actuators and sensors proposed for the default low-level control of the BSM1 (Gernaey et al., 2014). The state-space model

$$\dot{x}(t) = f(x(t), \tilde{u}(t), w(t)|\theta_x); \tag{34a}$$
$$\tilde{y}(t) = \tilde{g}(x(t)|\theta_y), \tag{34b}$$

has state variables $x(t) = ((x^{A(1)}, \cdots, x^{A(5)}), (x^{S(1)}, \cdots, x^{S(10)}))^\mathsf{T} \in \mathbb{R}^{N_x}_{\geq 0}$, measurements $\tilde{y}(t) = (S_O^{A(5)}, S_{NO}^{A(2)}, X_{SS}^{S(10)}, S_{NH}^{S(10)}, BOD_5^{S(10)}, COD^{S(10)}, N_{TOT}^{S(10)})^\mathsf{T} \in \mathbb{R}^{N_{\tilde{y}}}_{\geq 0}$, controls $\tilde{u}(t) = (Q_A, K_L a^{(5)})^\mathsf{T} \in \mathbb{R}^{N_{\tilde{u}}}_{\geq 0}$, and disturbances $w(t) = (Q_{IN}, x^{A(IN)})^\mathsf{T} \in \mathbb{R}^{N_w}_{\geq 0}$. The model consists of the original $N_x = 145$ state variables and $N_w = 14$ disturbances, but it has $N_{\tilde{u}} = 2$ controllable inputs and $N_{\tilde{y}} = 7$ measurements.

5.2.1. *Structural analysis*

The structural matrices $A_d \in \mathbb{R}^{N_x \times N_x}$, $B_d \in \mathbb{R}^{N_x \times N_{\tilde{u}}}$, and $C_d \in \mathbb{R}^{N_{\tilde{y}} \times N_x}$ are obtained from the Jacobians and the digraph $\mathcal{G}_d = (\mathcal{V}_d, \mathcal{E}_d)$, Fig. 11, has the vertex and edge sets

$$\begin{aligned}\mathcal{V}_d &= \mathcal{V}_{A_d} \cup \mathcal{V}_{B_d} \cup \mathcal{V}_{C_d} \\ &= \{x_1, \ldots, x_{N_x}\} \cup \{u_1, \ldots, u_{N_{\tilde{u}}}\} \cup \{y_1, \ldots, y_{N_{\tilde{y}}}\}; \\ \mathcal{E}_d &= \mathcal{E}_{A_d} \cup \mathcal{E}_{B_d} \cup \mathcal{E}_{C_d} \\ &= \{(x_{n_x}, x_{n'_x}) \mid [A_d]_{n'_x, n_x} \neq 0\} \cup \{(u_{n_u}, x_{n_x}) \mid [B_d]_{n_x, n_u} \neq 0\} \\ &\quad \cup \{(x_{n_x}, y_{n_y}) \mid [C_d]_{n_y, n_x} \neq 0\}.\end{aligned}$$

Controllability: The structural pair (A_d, B_d) associates with subgraph $\mathcal{G}_{d^c} = (\mathcal{V}_{d^c}, \mathcal{E}_{d^c})$, with $\mathcal{V}_{d^c} = \mathcal{V}_{A_d} \cup \mathcal{V}_{B_d}$ and $\mathcal{E}_{d^c} = \mathcal{E}_{A_d} \cup \mathcal{E}_{B_d}$. The topology of $\mathcal{G}_{d^c} = (\mathcal{V}_{d^c}, \mathcal{E}_{d^c})$ indicates that (A_d, B_d) is structurally controllable (Lemma 3).

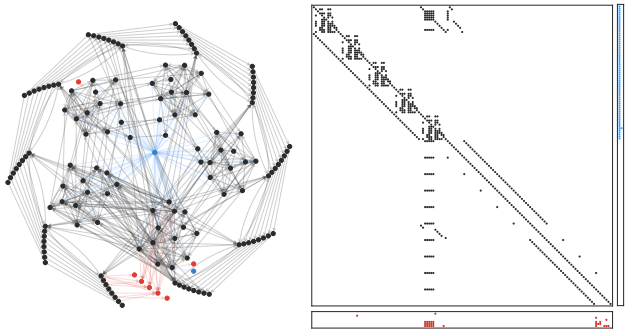

Figure 11: Network $\mathcal{G}_d = (\mathcal{V}_d, \mathcal{E}_d)$ associated to (A_d, B_d, C_d) (left and right panels, respectively). State vertices $x_{n_x} \in \mathcal{V}_A$ are in black, input vertices $u_{n_u} \in \mathcal{V}_B$ are in blue, and output vertices $y_{n_y} \in \mathcal{V}_C$ are in red. State-state edges $(x_{n_x}, x_{n'_x}) \in \mathcal{E}_A$, input-state edges $(u_{n_u}, x_{n_x}) \in \mathcal{E}_B$, and state-output edges $(x_{n_x}, y_{n_y}) \in \mathcal{E}_C$ are dyed to match the corresponding entries in (A_d, B_d, C_d). The state self-loops have been omitted.

The accessibility condition is satisfied with all state vertices reachable from a control vertex, with all state vertexes reachable through directed paths starting from the control vertex Q_A. The dilation-free condition is satisfied through a perfect matching $\mathcal{M}$ of size $|\mathcal{M}| = N_x$ formed by choosing every state vertex's self-loop, thus leaving no vertex unmatched. A perfect matching such as $\mathcal{M}$ ensures the dilation-free condition and suggests that controls are only needed to ensure accessibility. This implies that the state can be controlled by manipulating only the internal recirculation and then relying on self-dynamics to reach any state in the state-space. Though formally correct, such control strategy is clearly nonviable.

The topology of $\mathcal{G}_{d^c} = (\mathcal{V}_{d^c}, \mathcal{E}_{d^c})$ also shows that (A_d, B_d) is not strongly structurally controllable: It is not possible to find a colouring for both graph $\mathcal{G}_{d^c} = (\mathcal{V}_{d^c}, \mathcal{E}_{d^c})$ and modified graph $\widetilde{\mathcal{G}}_{d^c} = (\mathcal{V}_{d^c}, \widetilde{\mathcal{E}}_{d^c})$ in which all state vertices $x_{n_x} \in \mathcal{V}_A$ are coloured (Lemma 5). Being strongly structurally uncontrollable, there exist certain realisations of A_d and B_d for which the system is not controllable in a classical sense.

Observability: The structural pair (A_d, C_d) associates with subgraph $\mathcal{G}_{d^o} = (\mathcal{V}_{d^o}, \mathcal{E}_{d^o})$, with $\mathcal{V}_{d^o} = \mathcal{V}_{A_d} \cup \mathcal{V}_{C_d}$ and $\mathcal{E}_{d^o} = \mathcal{E}_{A_d} \cup \mathcal{E}_{C_d}$. The topology of $\mathcal{G}_{d^o} = (\mathcal{V}_{d^o}, \mathcal{E}_{d^o})$ indicates that pair (A_d, C_d) is structurally unobservable (Lemma 4). Similarly to the original configuration, no paths starting from state vertices $\{S_{ALK}^{A(r)}\}_{r=1}^{5}$, $\{S_{ALK}^{S(l)}\}_{l=1}^{10}$ and $\{S_O^{S(l)}\}_{l=7}^{10}$

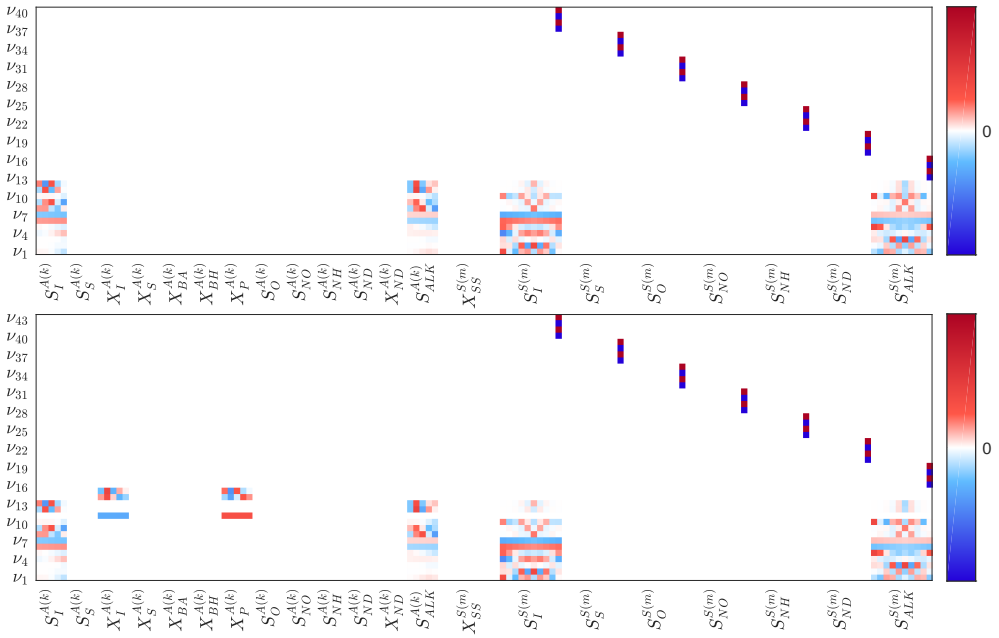

Figure 12: System $(A_d^{SS}, B_d^{SS}, C_d^{SS})$: Eigenvectors $v_i(\lambda_i)$ associated with $\lambda_i \in \sigma(A_d^{SS})$ failing the PBH controllability test ($\mathrm{rank}([\lambda_i I - A_d^{SS} \; B_d^{SS}]) < N_x$), top, and with $\lambda_i \in \sigma(A_d^{SS})$ failing the PBH observability test ($\mathrm{rank}([\lambda_i I - A_d^{SS^\mathsf{T}} \; C_d^{SS^\mathsf{T}}]^\mathsf{T}) < N_x$), bottom.

reach any of the output vertices. The accessibility condition is therefore not satisfied. Conversely, the dilation-free condition is still satisfied through a perfect matching $\mathcal{M}$ of size $|\mathcal{M}| = N_x$ formed by choosing every state vertex's self-loop. As expected, the topology of $\mathcal{G}_{d^o} = (\mathcal{V}_{d^o}, \mathcal{E}_{d^o})$ also indicates that (A_d, C_d) is also not strongly structurally observable.

5.2.2. *Classical analysis*

The numerical linearisation $(A_d^{SS}, B_d^{SS}, C_d^{SS})$ is obtained for the fixed point $SS \equiv (x^{SS}, u^{SS}, w^{SS}, y^{SS})$ in Gernaey et al. (2014) from the Jacobians evaluated at SS, to get $A_d^{SS} = \partial f/\partial x|_{SS}$, $B_d^{SS} = \partial f/\partial \tilde{u}|_{SS}$, and $C_d^{SS} = \partial \tilde{g}/\partial x|_{SS}$.

Controllability: Based on the PBH controllability test (Lemma 1), the pair (A_d^{SS}, B_d^{SS}) is not full-state controllable, as five complex conjugated pairs of eigenvalues with algebraic multiplicity equal to two and two real eigenvalues with algebraic multiplicities equal to two and twenty-eight, respectively, leads to rank-deficient matrices $[\lambda_i I - A_d^{SS} \; B_d^{SS}]$. The forty associated eigenvectors are shown in Fig. 12, top.

Note that the eigenvectors associated to the real eigenvalue with multiplicity equal to twenty-eight have non-zero entries at state variables relative to soluble matter in the settler's last layer, as already observed in Fig. 7. The other twelve eigenvectors have non-zero entries only on state variables $\{S_I^{A(r)}, S_{ALK}^{A(r)}\}_{r=1}^{5}$ and $\{S_I^{S(l)}, S_{ALK}^{S(l)}\}_{l=1}^{10}$. We conclude that, for the activated sludge plant described by the pair (A_d^{SS}, B_d^{SS}), it is not possible to design an input signal $\tilde{u}(t)$ that transfers the plant to a desired state, in finite time. Moreover, since A_d^{SS} is identical to the stable A^{SS}, all eigenvalues failing the PBH test satisfy $\mathrm{Re}(\lambda_i) < 0$ such that pair (A_d^{SS}, B_d^{SS}) is stabilizable (Lemma 8).

Observability: Based on he PBH observability test (Lemma 2), the pair (A_d^{SS}, C_d^{SS}) is not full-state observable, as ten distinct eigenvalues, including two real values with multiplicities equal to two and twenty-eight, respectively, and five complex conjugated pairs with multiplicities equal to two, lead to rank-deficient matrices $[\lambda_i I - A_d^{SS^\mathsf{T}} \; C_d^{SS^\mathsf{T}}]^\mathsf{T}$. The forty-three associated eigenvectors are in Fig. 12, bottom.

The nonzero entries of these eigenvectors relate to the same state variables as the nonzero entries of the eigenvectors previously observed on the PBH test of pair (A^{SS}, C^{SS}), Fig. 7. This implies that pair (A^{SS}, C^{SS}), with $N_y = 15$ outputs, and pair (A_d^{SS}, C_d^{SS}), with only $N_{\tilde{y}} = 7$ outputs, share the same observable subspace. Because A_d^{SS} is identical to the stable A^{SS}, all eigenvalues failing the PBH test satisfy $\mathrm{Re}(\lambda_i) < 0$ so that pair (A_d^{SS}, C_d^{SS}) is detectable (Lemma 9).

5.2.3. *Results*

We conclude that for the activated sludge plant given by Eq. (34) it is possible to design a control $\tilde{u}(t)$ that transfers the plant to a desired state, in finite time, for almost any possible realisation of (A_d, B_d). It is not possible, however, to determine the initial state $x(0)$, and thus neither intermediate states $x(t)$, starting from a measurement $\tilde{y}(t_f)$. Thus, it is also not possible to design a full-state-observer based on existing measurements, no matter what realisation of (A_d, C_d) is used. As for the specific linearisation $(A_d^{SS}, B_d^{SS}, C_d^{SS})$, it is neither controllable nor observable in the classical sense.

6. Concluding remarks

The dynamical properties of a model describing a common class of activated sludge plants are analysed, in a structural and a classical sense. We discuss the capabilities and limitations of the control and estimation tasks for activated sludge plants described by the Benchmark Simulated Model no. 1. The analysis is meant to provide a backbone for the design of efficient model-based controllers of activated sludge plants.

Our analyses show that activated sludge plants described by the BSM1 in Eq. (5) are full-state controllable but they are not observable, in a structural sense. Our results show that the plant is neither controllable nor it is observable in a strong structural sense. Formally, it is thus possible to determine a sequence of control actions that are capable to transfers the state of the system to any desired point in the state-space, from any initial state, in finite time, and for almost any realisation. However, it is also not possible to determine the initial state of the system, and thus neither its intermediate states, from a finite sequence of measurements. That is, it is also not possible to design a state-observer over the entire state-space.

For a linear approximation of the model which is commonly used in the literature, we studied the stability, controllability and observability, in a conventional sense. Under such realisation, we found that this system is stable, but it is not full-state controllable and it is not full-state observable. However, being stable, the system is both stabilisable and detectable. Energy-related metrics based on this linearisation show that the effort required to control and observe the system is very large. These efforts are among the lowest if biomass and particulate inert matter in the bio-reactors are directly controlled or measured. As actuation and sensing devices capable to directly control or measure these variables are practically unfeasible, these strategies are virtually inviable. Finally, a compound energy-related analysis shows that controlling and observing the BSM1 are high-demanding tasks even for a minimal and yet controllable and observable realisation.

The analysis of this class of activated sludge plants is extended on two alternative configurations of the system. We considered a reduced automation setup and a reduced-order model for the settler. For the first configuration, we found that the system is controllable but not observable in a structural sense, and that it is neither controllable nor observable in a conventional sense. For the second configuration, we found that this system is controllable but it is not observable in a structural sense. In this case, however, the system is controllable in a conventional sense, under the usual linearisation.

7. Acknowledgments

This study was done within the project Control4Reuse, part of the IC4WATER programme of the Water Challenges for a Changing World Joint Programme Initiative (Water JPI). The authors thank FUNCAP for the support within this initiative.

References

Alex, J., Tschepetzki, R., Jumar, U., 2002. Predictive control of nitrogen removal in WWTP using parsimonious models, in: Proceedings of the Fifteenth IFAC World Congress on Automatic Control, Barcelona, Spain. pp. 1458–1458.

Åmand, L., Olsson, G., Carlsson, B., 2013. Aeration control - A review. Water Science & Technology 67, 2374–2398.

Benazzi, F., Katebi, R., 2005. Nonlinear observability of activated sludge process models. IFAC Proceedings Volumes 38, 185–190. 16th IFAC World Congress.

Benner, P., Li, J.R., Penzl, T., 2008. Numerical solution of large-scale Lyapunov equations, Riccati equations, and linear-quadratic optimal control problems. Numerical Linear Algebra with Applications 15, 755–777.

Bof, N., Baggio, G., Zampieri, S., 2017. On the role of network centrality in the controllability of complex networks. IEEE Transactions on Control of Network Systems 4, 643–653.

Busch, J., Elixmann, D., Kühl, P., Gerkens, C., Schlöder, J.P., Bock, H.G., Marquardt, W., 2013. State estimation for large-scale wastewater treatment plants. Water Research 47, 4774–4787.

Callier, F.M., Desoer, C.A., 1991. Linear System Theory. Springer Texts in Electrical Engineering, Springer Science & Business Media.

Cormen, T.H., Leiserson, C.E., Rivest, R.L., Stein, C., 2009. Introduction to Algorithms. 3 ed., MIT Press.

Estrada, E., Knight, P.A., 2015. A First Course in Network Theory. Oxford University Press.

Francisco, M., Skogestad, S., Vega, P., 2015. Model predictive control for the self-optimized operation in wastewater treatment plants: Analysis of dynamic issues. Computers & Chemical Engineering 82, 259–272.

Gernaey, K., Jeppsson, U., Vanrolleghem, P., Copp, J., 2014. Benchmarking of Control Strategies for Wastewater Treatment Plants. Scientific and Technical Report Series No. 23, IWA Publishing.

Hall, P., 1935. On representatives of subsets. Journal of the London Mathematical Society s1-10, 26–30.

Han, H.G., Qian, H.H., Qiao, J.F., 2014. Nonlinear multiobjective model-predictive control scheme for wastewater treatment process. Journal of Process Control 24, 47–59.

Hautus, M.L.J., 1970. Stabilization, controllability and observability of linear autonomous systems. Indagationes Mathematicae (Proceedings) 73, 448–455.

Henze, M., Gujer, W., Mino, T., van Loosdrecht, M.C.M., 2000. Activated Sludge Models ASM1, ASM2, ASM2d and ASM3. Scientific and Technical Report Series No. 9, IWA Publishing.

Holenda, B., Dokomosa, E., Rèdey, A., Fazakas, J., 2008. Dissolved oxygen control of the activated sludge wastewater treatment process using model predictive control. Computers & Chemical Engineering 33, 1270–1278.

Jarczyk, J.C., Svaricek, F., Alt, B., 2011. Strong structural controllability of linear systems revisited, in: 50th IEEE Conference on Decision and Control and European Control Conference, pp. 1213–1218.

Jia, J., van Waarde, H.J., Trentelman, H.L., Camlibel, M.K., 2021. A unifying framework for strong structural controllability. IEEE Transactions on Automatic Control 66, 391–398.

Kalman, R., 1960. On the general theory of control systems, in: IFAC Proceedings Volumes, pp. 491–502.

Kalman, R.E., 1963. Mathematical description of linear dynamical systems. Journal of the Society for Industrial and Applied Mathematics Series A Control 1, 152–192.

Lin, C.T., 1974. Structural controllability. IEEE Transactions on Automatic Control 19, 201–208.

Liu, Y.Y., Slotine, J.J., Barabási, A.L., 2011. Controllability of complex networks. Nature 473, 167–173.

Liu, Y.Y., Slotine, J.J., Barabási, A.L., 2013. Observability of complex systems. Proceedings of the National Academy of Sciences 110, 2460–2465.

Mayeda, H., Yamada, T., 1979. Strong structural controllability. SIAM Journal on Control and Optimization 17, 123–138.

Moliner-Heredia, R., Penarrocha-Alos, I., Sanchis-Llopis, R., 2019. Eco-

nomic model predictive control of wastewater treatment plants based on bsm1 using linear prediction models, in: IEEE 15th International Conference on Control and Automation (ICCA), pp. 73–78.

Müller, P.C., Weber, H.I., 1972. Analysis and optimization of certain qualities of controllability and observability for linear dynamical systems. Automatica 8, 237–246.

Neto, O.B.L., Mulas, M., Corona, F., 2020a. On the controllability of activated sludge plants, in: Proceedings of the 2020 European Control Conference, IEEE. pp. 581–586.

Neto, O.B.L., Mulas, M., Corona, F., 2020b. On the observability of activated sludge plants. IFAC-PapersOnLine 53, 16802–16807. 21th IFAC World Congress.

Olsson, G., Andrews, J., 1978. The dissolved oxygen profile - a valuable tool for control of the activated sludge process. Water Research 12, 985–1004.

Olsson, G., Carlsson, B., Comas, J., Copp, J., Gernaey, K., Ingildsen, P., Jeppsson, U., Kim, C., Rieger, L., Rodrìguez-Roda, I., Steyer, J., Takács, I., Vanrolleghem, P., Vargas, A., Yuan, Z., Åmand, L., 2013. Instrumentation, control and automation in wastewater - from London 1973 to Narbonne 2013. Water Science & Technology 69, 1372–1385.

Olsson, G., Eklund, K., Dahlqvist, K., Ulmgren, L., 1973. Control Problems in Wastewater Treatment Plants. Research Reports TFRT-3064, Department of Automatic Control, Lund Institute of Technology (LTH).

Olsson, G., Nielsen, M., Yuan, Z., Lynggaard-Jensen, A., Steyer, J., 2005. Instrumentation, Control and Automation in Wastewater Systems. IWA Publishing, London.

Ostace, G., Cristea, V., Agachi, P., 2011. Cost reduction of the wastewater treatment plant operation by MPC based on modified ASM1 with two-step nitrification/denitrification model. Computers & Chemical Engineering 35, 2469 – 2479.

Pasqualetti, F., Zampieri, S., Bullo, F., 2014. Controllability metrics, limitations and algorithms for complex networks. IEEE Transactions on Control of Network Systems 1, 40–52.

Reinschke, K.J., 1988. Multivariable Control: a Graph-theoretic Approach. Springer.

Rosen, C., Larsson, M., Jeppsson, U., Yuan, Z., 2002. A framework for extreme-event control in wastewater treatment. Water Science & Technology 45, 299–308.

Stare, A., Vrečko, D., Hvala, N., Strmčnik, S., 2007. Comparison of control strategies for nitrogen removal in an activated sludge process in terms of operating costs: A simulation study. Water Research 41, 2004–2014.

Summers, T.H., Cortesi, F.L., Lygeros, J., 2016. On submodularity and controllability in complex dynamical networks. IEEE Transactions on Control of Network Systems 3, 91–101.

Takács, I., Patry, G., Nolasco, D., 1991. A dynamic model of the clarification-thickening process. Water Research 25, 1263–1271.

Van Dooren, P., 1981. The generalized eigenstructure problem in linear system theory. IEEE Transactions on Automatic Control 26, 111–129.

Yin, X., Decardi-Nelson, B., Liu, J., 2018. Subsystem decomposition and distributed moving horizon estimation of wastewater treatment plants. Chemical Engineering Research and Design 134, 405 – 419.

Yin, X., Liu, J., 2018. State estimation of wastewater treatment plants based on model approximation. Computers & Chemical Engineering 111, 79–91.

Yin, X., Liu, J., 2019. Subsystem decomposition of process networks for simultaneous distributed state estimation and control. AIChE Journal 65, 904–914.

Zeng, J., Liu, J., 2015. Economic model predictive control of wastewater treatment processes. Industrial & Engineering Chemistry Research 54, 5710–5721.

Zeng, J., Liu, J., Zou, T., Yuan, D., 2016. Distributed extended kalman filtering for wastewater treatment processes. Industrial & Engineering Chemistry Research 55, 7720–7729.

Zhang, A., Liu, J., 2019. Economic mpc of wastewater treatment plants based on model reduction. Processes 7, 682.

Zhao, C., Wang, W.X., Liu, Y.Y., Slotine, J.J., 2015. Intrinsic dynamics induce global symmetry in network controllability. Scientific Reports 5.

A. The Benchmark Model No. 1: State-space, parameters, equilibrium point, and smoothification

The state-space model equations, alongside model parameters and complementary information, are provided for the BSM1.

A.1. Biological reactors

The dynamics within each r-th reactor, represented by the set of state variables $x^{A(r)}$ given in Section 2. For any $Z^{A(r)} \in x^{A(r)}$,

$$\dot{Z}^{A(r)} = \begin{cases} \dfrac{Q^{(r)}}{V^{A(r)}}\Big[Z^{A(r-1)} - Z^{A(r)}\Big] - \dfrac{Q^{(r)}_{EC}}{V^{A(r)}} Z^{A(r)} + R_{Z^{A(r)}} & (r = 2, \cdots, 5) \\ \dfrac{1}{V^{A(1)}}\Big[Q_{IN} Z^{A(IN)} + Q_A Z^{A(5)} + Q_R Z^{S(1)}\Big] - \dfrac{Q^{(1)} + Q^{(1)}_{EC}}{V^{A(1)}} Z^{A(1)} + R_{Z^{A(1)}} & (r = 1) \end{cases} \tag{35}$$

where $Q^{(r)} = (Q_{IN} + Q_A + Q_R + \sum_{j=1}^{r-1} Q^{(j)}_{EC})$, for all $r = 1, \cdots, 5$, and $R_{Z^{A(r)}}$ is the contribution from reactions associated to component $Z^{A(r)}$ (Henze et al., 2000). Whenever $Z^{A(r)} = S_O^{A(r)}$ we add the term $K_L a^{(r)}[S_O^{sat} - S_O^{A(r)}]$ for both cases in Eq. (35). When $Z^{A(r)} = S_S^{A(r)}$ we add $(Q^{(r)}_{EC}/V^{A(r)})S_S^{EC}$, for both cases in Eq. (35).

The dynamics of the concentrations in reactors $r = 2, \cdots, 5$ are given by the set of differential equations

$$\dot{S}_I^{A(r)} = \frac{Q^{(r)}}{V^{A(r)}}\Big[S_I^{A(r-1)} - S_I^{A(r)}\Big] - \frac{Q^{(r)}_{EC}}{V^{A(r)}} S_I^{A(r)} \tag{36}$$

$$\begin{aligned} \dot{S}_S^{A(r)} = {} & \frac{Q^{(r)}}{V^{A(r)}}\Big[S_S^{A(r-1)} - S_S^{A(r)}\Big] + \frac{Q^{(r)}_{EC}}{V^{A(r)}}\Big[S_S^{EC} - S_S^{A(r)}\Big] \\ & - \frac{\mu_H}{Y_H} \frac{S_S^{A(r)}}{K_S + S_S^{A(r)}}\Big[\frac{S_O^{A(r)}}{K_{OH} + S_O^{A(r)}} + \eta_g \frac{K_{OH}}{K_{OH} + S_O^{A(r)}} \frac{S_{NO}^{A(r)}}{K_{NO} + S_{NO}^{A(r)}}\Big] X_{BH}^{A(r)} \\ & + k_h \frac{X_S^{A(r)}}{K_X X_{BH}^{A(r)} + X_S^{A(r)}}\Big[\frac{S_O^{A(r)}}{K_{OH} + S_O^{A(r)}} + \eta_h \frac{K_{OH}}{K_{OH} + S_O^{A(r)}} \frac{S_{NO}^{A(r)}}{K_{NO} + S_{NO}^{A(r)}}\Big] X_{BH}^{A(r)} \end{aligned} \tag{37}$$

$$\dot{X}_I^{A(r)} = \frac{Q^{(r)}}{V^{A(r)}}\Big[X_I^{A(r-1)} - X_I^{A(r)}\Big] - \frac{Q^{(r)}_{EC}}{V^{A(r)}} X_I^{A(r)} \tag{38}$$

$$\begin{aligned} \dot{X}_S^{A(r)} = {} & \frac{Q^{(r)}}{V^{A(r)}}\Big[X_S^{A(r-1)} - X_S^{A(r)}\Big] - \frac{Q^{(r)}_{EC}}{V^{A(r)}} X_S^{A(r)} \\ & - k_h \frac{X_S^{A(r)}}{K_X X_{BH}^{A(r)} + X_S^{A(r)}}\Big[\frac{S_O^{A(r)}}{K_{OH} + S_O^{A(r)}} + \eta_h \frac{K_{OH}}{K_{OH} + S_O^{A(r)}} \frac{S_{NO}^{A(r)}}{K_{NO} + S_{NO}^{A(r)}}\Big] X_{BH}^{A(r)} + \Big[1 - f_p\Big] b_H X_{BH}^{A(r)} + \Big[1 - f_p\Big] b_A X_{BA}^{A(r)} \end{aligned} \tag{39}$$

$$\begin{aligned} \dot{X}_{BH}^{A(r)} = {} & \frac{Q^{(r)}}{V^{A(r)}}\Big[X_{BH}^{A(r-1)} - X_{BH}^{A(r)}\Big] - \frac{Q^{(r)}_{EC}}{V^{A(r)}} X_{BH}^{A(r)} \\ & + \mu_H \frac{S_S^{A(r)}}{K_S + S_S^{A(r)}}\Big[\frac{S_O^{A(r)}}{K_{OH} + S_O^{A(r)}} + \eta_g \frac{K_{OH}}{K_{OH} + S_O^{A(r)}} \frac{S_{NO}^{A(r)}}{K_{NO} + S_{NO}^{A(r)}}\Big] X_{BH}^{A(r)} - b_H X_{BH}^{A(r)} \end{aligned} \tag{40}$$

$$\dot{X}_{BA}^{A(r)} = \frac{Q^{(r)}}{V^{A(r)}}\Big[X_{BA}^{A(r-1)} - X_{BA}^{A(r)}\Big] - \frac{Q^{(r)}_{EC}}{V^{A(r)}} X_{BA}^{A(r)} + \mu_A \frac{S_{NH}^{A(r)}}{K_{NH} + S_{NH}^{A(r)}} \frac{S_O^{A(r)}}{K_{OA} + S_O^{A(r)}} X_{BA}^{A(r)} - b_A X_{BA}^{A(r)} \tag{41}$$

$$\dot{X}_P^{A(r)} = \frac{Q^{(r)}}{V^{A(r)}}\Big[X_P^{A(r-1)} - X_P^{A(r)}\Big] - \frac{Q^{(r)}_{EC}}{V^{A(r)}} X_P^{A(r)} + f_P\Big[b_H X_{BH}^{A(r)} + b_A X_{BA}^{A(r)}\Big] \tag{42}$$

$$\begin{aligned} \dot{S}_O^{A(r)} = {} & \frac{Q^{(r)}}{V^{A(r)}}\Big[S_O^{A(r-1)} - S_O^{A(r)}\Big] - \frac{Q^{(r)}_{EC}}{V^{A(r)}} S_O^{A(r)} + K_L a^{(r)}\Big[S_O^{sat} - S_O^{A(r)}\Big] \\ & - \frac{1 - Y_H}{Y_H} \mu_H \frac{S_S^{A(r)}}{K_S + S_S^{A(r)}} \frac{S_O^{A(r)}}{K_{OH} + S_O^{A(r)}} X_{BH}^{A(r)} - \frac{4.57 - Y_A}{Y_A} \mu_A \frac{S_{NH}^{A(r)}}{K_{NH} + S_{NH}^{A(r)}} \frac{S_O^{A(r)}}{K_{OA} + S_O^{A(r)}} X_{BA}^{A(r)} \end{aligned} \tag{43}$$

$$\dot{S}_{NO}^{A(r)} = \frac{Q^{(r)}}{V^{A(r)}}\Big[S_{NO}^{A(r-1)} - S_{NO}^{A(r)}\Big] - \frac{Q_{EC}^{(r)}}{V^{A(r)}}S_{NO}^{A(r)} \tag{44}$$
$$- \frac{1-Y_H}{2.86Y_H}\mu_H \frac{S_S^{A(r)}}{K_S + S_S^{A(r)}}\frac{K_{OH}}{K_{OH}+S_O^{A(r)}}\frac{S_{NO}^{A(r)}}{K_{NO}+S_{NO}^{A(r)}}\eta_g X_{BH}^{A(r)} + \frac{\mu_A}{Y_A}\frac{S_{NH}^{A(r)}}{K_{NH}+S_{NH}^{A(r)}}\frac{S_O}{K_{OA}+S_O^{A(r)}}X_{BA}^{A(r)}$$

$$\dot{S}_{NH}^{A(r)} = \frac{Q^{(r)}}{V^{A(r)}}\Big[S_{NH}^{A(r-1)} - S_{NH}^{A(r)}\Big] - \frac{Q_{EC}^{(r)}}{V^{A(r)}}S_{NH}^{A(r)} \tag{45}$$
$$- \mu_H \frac{S_S}{K_S + S_S^{A(r)}}\Big[\frac{S_O^{A(r)}}{K_{OH}+S_O^{A(r)}} + \eta_g \frac{K_{OH}}{K_{OH}+S_O^{A(r)}}\frac{S_{NO}^{A(r)}}{K_{NO}+S_{NO}^{A(r)}}\Big] i_{XB} X_{BH}^{A(r)}$$
$$- \mu_A\Big(i_{XB} + \frac{1}{Y_A}\Big)\frac{S_{NH}^{A(r)}}{K_{NH}+S_{NH}^{A(r)}}\frac{S_O^{A(r)}}{K_{OA}+S_O^{A(r)}}X_{BA}^{A(r)} + k_a S_{ND}^{A(r)} X_{BH}^{A(r)}$$

$$\dot{S}_{ND}^{A(r)} = \frac{Q^{(r)}}{V^{A(r)}}\Big[S_{ND}^{A(r-1)} - S_{ND}^{A(r)}\Big] - \frac{Q_{EC}^{(r)}}{V^{A(r)}}S_{ND}^{A(r)} \tag{46}$$
$$- k_a S_{ND}^{A(r)} X_{BH}^{A(r)} + k_h \frac{X_{ND}^{A(r)} X_{BH}^{A(r)}}{K_X X_{BH}^{A(r)} + X_S^{A(r)}}\Big[\frac{S_O^{A(r)}}{K_{OH}+S_O^{A(r)}} + \eta_h \frac{K_{OH}}{K_{OH}+S_O^{A(r)}}\frac{S_{NO}^{A(r)}}{K_{NO}+S_{NO}^{A(r)}}\Big]$$

$$\dot{X}_{ND}^{A(r)} = \frac{Q^{(r)}}{V^{A(r)}}\Big[X_{ND}^{A(r-1)} - X_{ND}^{A(r)}\Big] - \frac{Q_{EC}^{(r)}}{V^{A(r)}}X_{ND}^{A(r)} \tag{47}$$
$$- k_h \frac{X_{ND}^{A(r)}}{K_X X_{BH}^{A(r)} + X_S^{A(r)}}\Big[\frac{S_O^{A(r)}}{K_{OH}+S_O^{A(r)}} + \eta_h \frac{K_{OH}}{K_{OH}+S_O^{A(r)}}\frac{S_{NO}^{A(r)}}{K_{NO}+S_{NO}^{A(r)}}\Big] X_{BH}^{A(r)}$$
$$+ b_H\Big(i_{XB} - f_P i_{XP}\Big)X_{BH}^{A(r)} + b_A\Big(i_{XB} - f_P i_{XP}\Big)X_{BA}^{A(r)}$$

$$\dot{S}_{ALK}^{A(r)} = \frac{Q^{(r)}}{V^{A(r)}}\Big[S_{ALK}^{A(r-1)} - S_{ALK}^{A(r)}\Big] - \frac{Q_{EC}^{(r)}}{V^{A(r)}}S_{ALK}^{A(r)} \tag{48}$$
$$- \frac{i_{XB}}{14}\mu_H \frac{S_S^{A(r)}}{K_S + S_S^{A(r)}}\frac{S_O^{A(r)}}{K_{OH}+S_O^{A(r)}}X_{BH}^{A(r)} + \frac{1}{14}k_a S_{ND}^{A(r)} X_{BH}^{A(r)}$$
$$+ \Big(\frac{1-Y_H}{14\times 2.86Y_H} - \frac{i_{XB}}{14}\Big)\mu_H \frac{S_S^{A(r)}}{K_S + S_S^{A(r)}}\frac{K_{OH}}{K_{OH}+S_O^{A(r)}}\frac{S_{NO}^{A(r)}}{K_{NO}+S_{NO}^{A(r)}}\eta_g X_{BH}^{A(r)}$$
$$- \Big(\frac{i_{XB}}{14} + \frac{1}{7Y_A}\Big)\mu_A \frac{S_{NH}^{A(r)}}{K_{NH}+S_{NH}^{A(r)}}\frac{S_O^{A(r)}}{K_{OA}+S_O^{A(r)}}X_{BA}^{A(r)}$$

A.2. Secondary settler

The dynamics for suspended solids in each l-th settler's layer, $X_{SS}^{S(l)}$, are described by

$$\dot{X}_{SS}^{S(l)} = \begin{cases} \dfrac{Q_e}{V^{S(l)}}\Big[X_{SS}^{S(l-1)} - X_{SS}^{S(l)}\Big] - \dfrac{1}{h^{S(l)}}J_{cla}\Big(X_{SS}^{S(l)}, X_{SS}^{S(l-1)}\Big) & (l=10) \\ \dfrac{Q_e}{V^{S(l)}}\Big[X_{SS}^{S(l-1)} - X_{SS}^{S(l)}\Big] + \dfrac{1}{h^{S(l)}}\Big[J_{cla}\Big(X_{SS}^{S(l+1)}, X_{SS}^{S(l)}\Big) - J_{cla}\Big(X_{SS}^{S(l)}, X_{SS}^{S(l-1)}\Big)\Big] & (l=7,\cdots,9) \\ \dfrac{Q_f}{V^{S(l)}}\Big[X_f - X_{SS}^{S(l)}\Big] + \dfrac{1}{h^{S(l)}}\Big[J_{cla}\Big(X_{SS}^{S(l+1)}, X_{SS}^{S(l)}\Big) - J_{st}\Big(X_{SS}^{S(l)}, X_{SS}^{S(l-1)}\Big)\Big] & (l=6) \\ \dfrac{Q_u}{V^{S(l)}}\Big[X_{SS}^{S(l+1)} - X_{SS}^{S(l)}\Big] + \dfrac{1}{h^{S(l)}}\Big[J_{st}\Big(X_{SS}^{S(l+1)}, X_{SS}^{S(l)}\Big) - J_{st}\Big(X_{SS}^{S(l)}, X_{SS}^{S(l-1)}\Big)\Big] & (l=2,\cdots,5) \\ \dfrac{Q_u}{V^{S(l)}}\Big[X_{SS}^{S(l+1)} - X_{SS}^{S(l)}\Big] + \dfrac{1}{h^{S(l)}}J_{st}\Big(X_{SS}^{S(l+1)}, X_{SS}^{S(l)}\Big) & (l=1) \end{cases}$$

The dynamics of soluble matter $\dot{S}_{(\cdot)}^{S(l)}$ within each l-th layer is

$$\dot{S}_{(\cdot)}^{S(l)} = \begin{cases} \dfrac{Q_e}{V^{S(l)}}\left[S_{(\cdot)}^{S(l-1)} - S_{(\cdot)}^{S(l)}\right] & (l = 7, \cdots, 10); \\ \dfrac{Q_f}{V^{S(l)}}\left[S_{(\cdot)}^{A(5)} - S_{(\cdot)}^{S(l)}\right] & (l = 6); \\ \dfrac{Q_u}{V^{S(l)}}\left[S_{(\cdot)}^{S(l+1)} - S_{(\cdot)}^{S(l)}\right] & (l = 1, \cdots, 5), \end{cases} \tag{49}$$

with $X_f = 0.75\left(X_I^{A(5)} + X_S^{A(5)} + X_{BH}^{A(5)} + X_{BA}^{A(5)} + X_P^{A(5)}\right)$, $Q_f = (Q_{IN} + Q_R)$, $Q_u = (Q_R + Q_W)$, and $Q_e = (Q_{IN} - Q_W)$.

The downward and upward flux of solids are respectively given by

$$J_{st}\left(X_{SS}^{S(l)}, X_{SS}^{S(l-1)}\right) = \min\left[v_s\left(X_{SS}^{S(l-1)}\right)X_{SS}^{S(l-1)}, v_s\left(X_{SS}^{S(l)}\right)X_{SS}^{S(l)}\right]; \tag{50}$$

$$J_{cla}\left(X_{SS}^{S(l)}, X_{SS}^{S(l-1)}\right) = \begin{cases} \min\left[v_s\left(X_{SS}^{S(l-1)}\right)X_{SS}^{S(l-1)}, v_s\left(X_{SS}^{S(l)}\right)X_{SS}^{S(l)}\right] & \text{if } X_{SS}^{S(l-1)} > X_t; \\ v_s\left(X_{SS}^{S(l)}\right)X_{SS}^{S(l)} & \text{otherwise,} \end{cases} \tag{51}$$

in which

$$v_s\left(X_{SS}^{S(l)}\right) = \max\left\{0, \min\left[v_0^{max}, v_0\left(e^{-r_h(X_{SS}^{S(l)} - f_{ns}X_f)} - e^{-r_p(X_{SS}^{S(l)} - f_{ns}X_f)}\right)\right]\right\}. \tag{52}$$

A.3. Smoothification of discontinuities

Jacobian linearisations require the functions $f(\cdot)$ and $g(\cdot)$ to be differentiable with respect to the state variables and the inputs. Due to the discontinuities in the model of the settler, this is not true for the BSM1. A smooth approximation of the original model was obtained by replacing the terms corresponding to minimum and maximum functions between two terms by a log-sum-exp or softmax function, whereas a hyperbolic tangent function was used for approximating conditional statements.

We rewrite the condition for the downward flux of solids, $J_{cla}(\cdot)$ from Eq. (51), as

$$J_{cla}(\cdot) = \varphi(X_{SS}^{S(l-1)})\min\left[v_s\left(X_{SS}^{S(l-1)}\right)X_{SS}^{S(l-1)}, v_s\left(X_{SS}^{S(l)}\right)X_{SS}^{S(l)}\right] + \left[1 - \varphi(X_{SS}^{S(l-1)})\right]v_s\left(X_{SS}^{S(l)}\right)X_{SS}^{S(l)}$$

with $\varphi(X_{SS}^{S(l-1)}) = 1$ when $X_{SS}^{S(l-1)} - X_t > 0$ and $\varphi(X_{SS}^{S(l-1)}) = 0$ otherwise.

We approximate the step function $\varphi(X_{SS}^{S(l-1)})$ with an hyperbolic tangent function

$$\varphi(X_{SS}^{S(l-1)}) \approx 0.5 + 0.5\tanh\left(50\left(X_{SS}^{S(l-1)} - X_t\right)\right).$$

A.4. Model parameters

The model equations depend on the set of stoichiometric, kinetic and general parameters described in Table 3.

Table 3
Benchmark Model No. 1: Model constant parameters.

	Stoichiometric parameter	Value	Units
Y_A	Autotrophic yield	0.24	g X_{BA} COD formed · (g N oxidised)$^{-1}$
Y_H	Heterotrophic yield	0.67	g X_{BH} COD formed · (g COD utilised)$^{-1}$
f_P	Fraction of biomass to particulate products	0.08	g X_P COD formed · (g X_{BH} decayed)$^{-1}$
i_{XB}	Fraction nitrogen in biomass	0.08	g N (g COD)$^{-1}$ in biomass
i_{XP}	Fraction nitrogen in particulate products	0.06	g N (g COD)$^{-1}$ in X_P

	Kinetic parameter	Value	Units
μ_H	Maximum heterotrophic growth rate	4.00	d^{-1}
K_S	Half-saturation (heterotrophic growth)	10.0	g COD m^{-3}
K_{OH}	Half-saturation (heterotrophic oxygen)	0.20	g O_2 m^{-3}
K_{NO}	Half-saturation (nitrate)	0.50	g NO_3-N m^{-3}
b_H	Heterotrophic decay rate	0.30	d^{-1}
ν_g	Anoxic growth rate correction factor	0.80	dimensionless
ν_h	Anoxic hydrolysis rate correction factor	0.80	dimensionless
k_h	Maximum specific hydrolysis rate	3.00	g X_S (g X_{BH} COD d)$^{-1}$
K_X	Half-saturation (hydrolysis)	0.10	g X_S (g X_{BH} COD)$^{-1}$
μ_A	Maximum autotrophic growth rate	0.50	d^{-1}
K_{NH}	Half-saturation (autotrophic growth)	1.00	g NH_4-N m^{-3}
b_A	Autotrophic decay rate	0.05	d^{-1}
K_{OA}	Half-saturation (autotrophic oxygen)	0.40	g O_2 m^{-3}
k_a	Ammonification rate	0.05	m^3 (g COD d)$^{-1}$

	Secondary settler parameter	Value	Units
v_0^{max}	Maximum settling velocity	250.0	m d^{-1}
v_0	Maximum Vesilind settling velocity	474.0	m d^{-1}
r_h	Hindered zone settling parameter	0.000576	m^3 (g SS)$^{-1}$
r_p	Flocculant zone settling parameter	0.00286	m^3 (g SS)$^{-1}$
f_{ns}	Non-settleable fraction	0.00228	dimensionless

	General parameter	Value	Units
$V^{A(1\rightsquigarrow 2)}$	Reactor volume (anoxic section)	1000	m^3
$V^{A(3\rightsquigarrow 5)}$	Reactor volume (aerobic section)	1333	m^3
$V^{S(l)}$	Settler layer volume	600	m^3
$h^{S(l)}$	Settler layer height	0.4	m
S_S^{EC}	External carbon source concentration	$4 \cdot 10^5$	g COD m^{-3}
S_O^{sat}	Oxygen saturation concentration	8.0	g O_2 m^{-3}
X_t	Settling threshold concentration	3000	g m^{-3}

A.5. Common equilibrium point for linearisation

The conventional operation corresponding to the steady-state point $SS := (x^{SS}, u^{SS}, w^{SS}, y^{SS})$ is presented in Table 4.

Table 4
Benchmark Model No. 1: Steady-state point $SS := (x^{SS}, u^{SS}, w^{SS}, y^{SS})$.

	Influent	Reactor					
	IN	A(1)	A(2)	A(3)	A(4)	A(5)	Units
S_I	30	30	30	30	30	30	g COD m^{-3}
S_S	69.5	2.81	1.46	1.15	0.995	0.889	g COD m^{-3}
X_I	51.2	1149	1149	1149	1149	1149	g COD m^{-3}
X_S	202.32	82.1	76.4	64.9	55.7	49.3	g COD m^{-3}
X_{BH}	28.17	2552	2553	2557	2559	2559	g COD m^{-3}
X_{BA}	0	148	148	149	150	150	g COD m^{-3}
X_P	0	449	450	450	451	452	g COD m^{-3}
S_O	0	0.0043	6.31E-5	1.72	2.43	0.491	g O_2 m^{-3}
S_{NO}	0	5.37	3.66	6.54	9.30	10.4	g N m^{-3}
S_{NH}	31.56	7.92	8.34	5.55	2.97	1.73	g N m^{-3}
S_{ND}	6.95	1.22	0.882	0.829	0.767	0.688	g N m^{-3}
X_{ND}	10.59	5.28	5.03	4.39	3.88	3.53	g N m^{-3}
S_{ALK}	7	4.93	5.08	4.67	4.29	4.13	mol HCO_3^- m^{-3}

	Settler Layer										
	S(1)	S(2)	S(3)	S(4)	S(5)	S(6)	S(7)	S(8)	S(9)	S(10)	Units
X_{SS}	6394	356.07	356.07	356.07	356.07	356.07	68.98	29.54	18.11	12.5	g COD m^{-3}
S_I	30	30	30	30	30	30	30	30	30	30	g COD m^{-3}
S_S	0.89	0.89	0.89	0.89	0.89	0.89	0.89	0.89	0.89	0.89	g COD m^{-3}
S_O	0.49	0.49	0.49	0.49	0.49	0.49	0.49	0.49	0.49	0.49	g O_2 m^{-3}
S_{NO}	10.42	10.42	10.42	10.42	10.42	10.42	10.42	10.42	10.42	10.42	g N m^{-3}
S_{NH}	1.73	1.73	1.73	1.73	1.73	1.73	1.73	1.73	1.73	1.73	g N m^{-3}
S_{ND}	0.69	0.69	0.69	0.69	0.69	0.69	0.69	0.69	0.69	0.69	g N m^{-3}
S_{ALK}	4.13	4.13	4.13	4.13	4.13	4.13	4.13	4.13	4.13	4.13	mol HCO_3^- m^{-3}

	Input	Units
Q_{IN}	18846	m^3 d^{-1}
Q_A	55338	m^3 d^{-1}
Q_R	18446	m^3 d^{-1}
Q_W	385	m^3
$K_L a^{(1)}$	0	d^{-1}
$K_L a^{(2)}$	0	d^{-1}
$K_L a^{(3)}$	240	d^{-1}
$K_L a^{(4)}$	240	d^{-1}
$K_L a^{(5)}$	84	d^{-1}
$Q_{EC}^{(1)}$	0	m^3 d^{-1}
$Q_{EC}^{(2)}$	0	m^3 d^{-1}
$Q_{EC}^{(3)}$	0	m^3 d^{-1}
$Q_{EC}^{(4)}$	0	m^3 d^{-1}
$Q_{EC}^{(5)}$	0	m^3 d^{-1}